ELECTRORHEOLOGY

Rheology is the science of the deformation and flow of matter. *Electrorheology* is concerned mostly with the electrorheological (ER) effect, which consists of a sudden change of apparent viscosity in a suspension of particles induced by an electric field. The first applications of this effect were patented in 1947 by Winslow after several years of detailed studies and observations (1,2). Hence, it is also named the *Winslow effect.* Winslow called his slurries electroviscous fluids, because electroviscous effects had been previously reported in other systems, although on a much smaller scale (3–5). In literature outside the US and Britain, the electroviscous term is sometimes still used as a synonym of electroheological, although this is not strictly correct from a microscopic point of view. In Russian literature, the ER effect is sometimes named the *Quincke effect.* A brief review of the early history and references on ER related phenomena can be found in Ref. 6.

Although even some homogeneous liquids exhibit weak electroviscous effects (3–6), only concentrated dispersions of solid particles in dielectric liquids provide ER effects strong enough to be of technological interest. Large viscosity changes require the application of strong electric fields, of the order of kilovolts per millimeter (kV/mm). A significant increase in viscosity takes only milliseconds and is caused by the tendency of the micrometer-size suspended particles to form fibrous structures in the directions of the applied electric field. The individual particles become polarized, attract one another, and form chains, which bundle into filaments, spanning the gap between the electrodes. The strength of these filaments enables the ER fluid to sustain stress. Eventually, the liquid suspension turns completely into a viscoelastic gellike solid. To make this structure flow again, while maintaining the electric field, requires applying shear stress, which breaks the filaments. The minimum shear stress needed to cause flow, called *yield stress,* is typically proportional to the magnitude squared of the applied electric field. The amount of force or torque that an ER device transmits is related to the yield stress, whose effect persists as increased viscosity even when the shear stress exceeds the yield stress and flow is forced. The ER effect is fully and even more rapidly reversible. When the applied electric field is turned off, particle polarization and the corresponding attraction immediately disappear, and the solidified or highly viscous fluid reverts almost instantly to the original low-viscosity liquid.

The response of an ER fluid is completely reversible and much faster than that of conventional mechanical systems. Hence, it offers great potential for high technology applications to engine mounts (actively controlling engine shake) and other vibration isolators, shock absorbers and other tunable dampers, nonslip fluid clutches and variable-differential transmissions, brakes, valves without moving parts, flow pumps, and various other fluidic control devices. The ER effect typically provides better control of fluid flow and power transmission and reduces the energy loss and damage due to vibrations (for example, through optimal control of a vehicle's vertical motion). In spite of that, commerical use of ER devices is still limited, in part because of the performance of currently available ER fluids. For example, the maximum strength of the yield stress seldom exceeds 5 kPa, which is insufficient for many applications. The corresponding need for large electric fields also requires that ER fluids be poor conductors of electricity, or power consumption and heat dissipation become excessive. This is a major problem for aqueous suspensions, most notably for dc applications. On the other hand, dispersed particles in low-conductivity liquids have a greater tendency to settle under gravitational and centrifugal fields (because of a lack of mobile charges that readily attach to particle surfaces and stabilize them against settling). Furthermore, for automotive use, ER fluids should remain stable and reliable for prolonged use and should sustain large temperature variations (from -50 to 150°C), chemical action, mechanical attrition, and wear.

A possible way to eliminate sedimentation is to match the densities of the particles and the medium. This is difficult for high-density particles, such as silica, but it may be achieved either by making insulating oils heavier by halogenation or by switching to lighter polymeric particles. Different thermal expansion coefficients between particles and medium typically allow a density match only at given temperatures, rather than over a wide temperature range (densities and thermal expansion coefficients can be matched only with special ternary liquid mixtures). In the absence of electrical charges or protective agents, particles generally tend to attract when close to each other (because of van der Waals forces) and may irreversibly coagulate when settling. Charge stabilization keeps the particles apart, but this typically requires media with unacceptably high conductivity, such as water. *Steric stabilization* provides substantial protection against cohesion through absorption or bonding of additives soluble in the fluid on the particle surfaces, such as *surfactants* or stabilizing polymer fragments. However, some surfactants act properly as stabilizers in the absence of electric fields but fail when high fields are applied (by allowing charge transfer between particles). Furthermore, surfactants are not readily available for anhydrous systems. On the other hand, block or graft copolymers appear more promising and versatile because their structures and chain lengths can be varied to sufficiently stabilize the particles, even when they are made of surfactant compounds (8). When stabilizing polymer fragments are relatively short, weak aggregates may still form, but they may be easily redispersed by stirring. The degree of reversible aggregation which can be tolerated depends on the ER application.

Brownian motion counters settling, but its effect is significant only for small submicron particles. Such size is sometime taken to define rather restrictively the range of *colloidal suspensions.* However, reduction in particle size decreases the yield stress and increases the response time. In fact, when effective, random Brownian forces disrupt alignment of particles into chains and filaments, thus weakening the ER effect. Given that, it is generally preferable to use particles large enough ($\sim$10 μm) that Brownian motion is negligible.

Particles of such dimensions in dilute suspensions are visible under a high-power optical microscope, that allows direct observation of their shape and size distribution. Filamentation induced by a strong electric field is discernible in such conditions (9–15). However, concentrated ER fluids (with particulate volume fractions between 0.2 and 0.6) are generally opaque. Then, the degree of aggregation at zero field or the structures that form at high fields are usually inferred from rheological measurements. Other electro-optical techniques can be used to determine directly the morphology of ER systems at light wavelengths where they are transparent. For example, Chen et al. (16) studied an ER suspension of relatively large diameter glass spheres (about 20 or 40 μm) in a silicone oil by using the transmitted pattern of a laser beam. They found that the ER solid formed under the applied electric field has a columnar body-centered tetragonal structure. In a similar experiment, Martin et al. used a different optical configuration and much smaller spheres (about 0.7 μm in diameter) in an index-matched medium to further study the dynamics of chain formation and their aggregation into columns (17). Various models which attempt to interpret the results of these experiments and other basic ER phenomena are described in two popular articles (18,19).

There are other systems analogous to ER fluids. Materials that are permanently ER solids (i.e., they do not flow under strain even at zero field) consist of particles frozen in elastomeric media. Application of an electric field increases the shear modulus of these composites. Various other *electroviscous effects* in sols, emulsions, and electrolyte systems are caused by internal electric fields produced by charged particles and free ions (20). Most notably, *magnetorheological* (MR) *fluids* consist of suspensions of ferromagnetic particles exhibiting under an applied magnetic field rheological changes analogous to ER fluids. In practical applications, MR fluids offer several advantages over ER fluids (21). For example, they are not limited by conduction or dielectric breakdown. Hence, conducting liquids, such a water, are not excluded. Purity is also not a problem. On the other hand, MR fluids have much longer response times than ER fluids, relax much more slowly, and retain residual magnetization. MR fluids also require typically larger and heavier power sources (magnets). Despite the great research and technological interest that ferrofluids currently enjoy, lack of space prevents any adequate treatment of this topic in this article. A general discussion can be found in Ref. 22. Recent advances are reported, for example, in Refs. 23 and 24.

COMPOSITION AND PROPERTIES OF ER FLUIDS

The ER effect was originally discovered in suspensions of starch and silica gel particles in natural, mineral, or lubricating oils (1,2). Many ER fluids have been based on similar particulates (such as cellulose, dextran, alginic acid, resins, metal oxides, clay minerals, talcum powder, gypsum) and dispersants (such as gasoline, kerosene, toluene). However, a significant amount of water (between 5% and 30%) is necessary for these dispersions to exhibit any appreciable ER effect. It is believed that water, repelled by the hydrophobic suspending liquid, collects on the surface of the hygroscopic particles. Dissolved salts in this envelope provide mobile ions that polarize in the (local) electric field. This substantially augments the particle's intrinsic polarization, even though the aqueous envelope may be very thin. Unfortunately, the presence of such conducting water increases power consumption and heat dissipation. It further makes the ER properties sensitive to moisture content, hence, subject to chemical, electrochemical, and thermal degradation. A second generation of less abrasive ER fluids based on softer polymer particles has been developed since the late 1970s, but most of these suspensions still require water to produce substantial ER activity (12,25).

Components frequently added to ER fluids to increase the ER effect are called *activators.* They presumably work by augmenting the intrinsic polarizability of the particles, although their effectiveness is not simply related to the resulting permittivities. The role of water as an activator has already been mentioned. Other additives that work by similar mechanisms are various alcohols, carbonates, and glycols. Although some of them are less volatile and less reactive than water, most of them are substantially less effective than water and also lead to undesirable conductivity and dissipation. Surfactants also play some role as activators, presumably through ionic conduction within the surfactant layer.

The inherent relationship between charge mobility and ER activity has been demonstrated quantitatively in photoelectrorheological fluids, based on photoconducting particles, such as phenothiazine. These fluids have greatly enhanced ER activity when they are exposed to light of the proper frequency, which greatly increases the number of free electronic charge carriers (26, 27).

Since the mid 1980s, a third generation of substantially anhydrous ER fluids, inherently more stable and effective at higher temperatures, has been introduced. The particles are made of polymers or semiconductors (28), or have a composite structure, with a conducting core and a chemically formed insulating thin-skin layer, which is needed to prevent electrical conduction between particles in contact in chains and filaments (29,30). Particle encapsulation may also serve to reduce particle attrition and chemical reactivity with the environment. Similarly, the particles may have a light polymer core and a double layer, consisting of an inner conducting shell and an outer insulating film (31,32). Carbonaceous particles and optically anisotropic spherules with insulating layers have also been used (33). Particles made of aluminosilicates dispersed in paraffin oil provide improved ER fluids substantially free of water (34). In this case, the polarization augmentation is produced by movement of intrinsic metal cations through cavities and channels within the highly porous zeolite particles, rather than by extrinsic ions of electrolytes typically dissociated by water (35). Polyelectrolyte particles, which commonly require water to function as ER fluids, presumably by dissociating the cations from the macroions, also function with greatly reduced amounts of water, if cations can

move within the confines of a chain coil (27, 36, 37). ER fluids completely free of water have also been reported (38).

Even truly homogeneous polymer solutions, such as poly (γ-benzyl-L-glutamate) in various solvents, are ER active. This highlights the great versatility and ubiquity of the ER effect and the variety and complexity of the microscopic mechanisms that produce it (27). In addition to the removal of water, the problems of settling and abrasion are eliminated with homogeneous solutions because there is no dispersed phase. However, some solvents are polar and cause high currents and power consumption, and some have disadvantages of greater toxicity, aggressiveness, and limited operating temperatures. These solutions may be in a liquid-crystal state, which may also contribute to their ER activity. Liquid crystals are generally more suitable for magnetorheological applications, but understanding the mechanisms of the ER effect in various types of liquid crystals is nonetheless important (39). Their ER activity results both from the high polarizability of polymer molecules in solution and from the alignment of their large permanent dipole moments with the electric field because the alignment of long rigid-rod polymer molecules perpendicular to the flow increases shear viscosity (40).

Currently, the most common ER fluids in commercial use are silicas and zeolites in silicone oils, which are preferable to mineral oils because they are usable over a broader temperature range. In research, new materials are constantly produced and investigated for ER effects, e.g., fullerenes (41).

A survey of the patent literature for material composition, that is, particles, dispersants, surfactants, and activators, of available ER fluids is provided in Table 2 of Ref. 6. A complete list of ER fluid and device patents issued up to 1991 is provided in Sec. 7.2 of Ref. 42. An earlier survey of ER fluids can be found in Table 1 of a review article by Block and Kelly (43). An update of that and a list of polymers used for the particulate dispersed phase are provided, respectively, in Tables 1 and 2 of Ref. 13. A chronology of ER fluid and device development is included in Ref. 44.

BASIC REQUIREMENTS FOR ENGINEERING AND COMMERCIAL APPLICATIONS OF ER FLUIDS

Given the advanced level of modern solid-state electronics and control circuitry, the development of reliable and inexpensive power supplies and computerized control systems for ER devices should not be an impediment to ER technology. However, low-cost commercial power/control systems that permit rapid (millisecond) switching at high voltages are unavailable. The design of specific devices is also not yet sufficiently refined to take full advantage of the unique characteristics of ER fluids, thus causing less than optimal performance in many applications. Nonetheless, the major obstacle to the development of ER technology seems to be the current unavailability of ER fluids capable of satisfying the demands for strongly competitive and commercializable units.

Improvements of ER fluids for technological applications are needed in the following areas, roughly in order of their critical importance and corresponding difficulty to attain (see also Refs. 13 and 42):

1. High strength (yield stress and especially shear stress under flow conditions), at relatively lower applied fields
2. Wide operating temperature range (set by mechanical energy dissipation or environment, such as in shock absorbers or engine mounts)
3. Low electrical power requirement and consumption, hence, low conductivity (which is harder to maintain at higher temperatures and for faster responding ER fluids)
4. Stability (overcoming settling of particles, particularly when the fluid stays inactivated in the gravitational field for extended periods or when used repeatedly in centrifugal fields)
5. Resistance to thermal, chemical, and mechanical degradation in prolonged use
6. Zero-field viscosity less than a poise (to minimize drag and unwanted mechanical energy dissipation).
7. High dielectric breakdown strength (which depends on the microscopic composition and configuration in any state of the system and limits the maximum electric field that can be applied)
8. No contaminants (which may strongly affect, for example, conductivity and dielectric breakdown strength through ionic dissociation)
9. No electrophoresis, no dynamic separation, and low volatility
10. No abrasive, corrosive, electrolytic, or oxidative degradation (over repetitive cycle duties) of any component of the fluid, electrodes, seals, and containers
11. Fast response time (adequate for most applications, but still limiting high-frequency ac fields)
12. Nontoxic, nonhazardous, nonflammable, disposable substances

No single ER fluid obviously meets all of these requirements for all possible applications. Each individual ER device has its own specifications, which leads to selecting a particular ER fluid. An overall measure of merit for an ER fluid is given by the *Winslow number,* which is the ratio between the power density inherent in the ER effect (defined as the ratio between the square of the yield stress and the zero-field viscosity) and the power density consumption (which is the product of the electric field times the current density). Current ER fluids achieve Winslow numbers over 10^3 but only within narrow temperature ranges. At higher temperatures, the power density consumption rises too much, and at lower temperatures the ER inherent power density becomes too low (45).

The variety of requirements for ER fluids and devices is easily illustrated by automotive applications. For instance, anhydrous ER fluids are difficult to shield from aqueous contamination in shock absorbers exposed to harsh environments. Engine mounts require ER fluids that retain stability over wide frequency and temperature ranges, but only a moderate yield stress (1 to 2 kPa) is needed. Conversely, clutches and most other similar applications require a substantially higher yield stress. One possibility of attaining the latter is to manufacture spheroidal or elongated particles and optimize their aspect ratio, that is, the ratio between principal axes. This has been suggested by simple dipolar estimates and demonstrated more convincingly by experiment (14). Unfortunately, the increase in shear strength with aspect ratio is mostly static and disappears with increasing shear rate

(46), under which clutches must also operate. Furthermore, longer response times are definitely involved, because elongated particles must rotate against their inertia and friction into alignment with the electric field. However, a somewhat slower ER response may be tolerable and even desirable for clutches to reduce mechanical shock.

For fluidic control systems there are two important concerns: (1) Filtration phenomena associated with pressure-driven flow in an ER valve may generate a difference between solvent and particle velocities, hence, cause dynamic separation. (2) Instabilities may arise in the flow of typically stable ER suspensions under electric fields that vary more rapidly in space and/or time.

Finally, safety, environmental, and cost considerations must also be taken into account because they restrict the applications of materials otherwise particularly ER effective. For instance, halogenated hydrocarbons are ideal dispersants for stability, density and cost, but are toxic, difficult to contain, and hard to dispose of. Silicone fluids are not toxic, but they are not biodegradable, and even traces of silicone contaminants ruin the appearance of surfaces repainted in autobody shops. A safety concern is the high voltage required in ER applications. Thus, ideal fluids should operate with very low current densities (below 1 $\mu A/cm^2$), so that current-limiting circuitry can be applied to protect against accidental shock to users. Unfortunately, current ER fluids cannot carry low current density and high yield stress at the same time (except, possibly, dry aluminosilicate particulate systems).

For profitable commercial products, ER active dampers on engines are the best candidates, followed by shock absorbers based on similar concepts (but more demanding on ER fluid performance). The feasibility of ER clutches has been demonstrated in various prototypes (by Lord Corporation and various other centers), but competitive mass production of an automotive ER clutch of reasonable dimensions, low power consumption, and low cost still requires considerable torque enhancement (i.e., a yield stress up to about 20 kPa) and some zero-field viscosity reduction (to minimize open-clutch drag) in the development of ER fluids. On the other hand, low-torque applications, such as automotive alternators, air conditioners, and other accessory drive clutches are already viable and advantageous because they permit full decoupling when the accessory is not in use. Continuously variable ER transmissions are of interest because they would allow maintaining engine speed at an optimal value, producing major energy savings. However, this is a future application, because it requires at least an order of magnitude improvement in ER fluids. Current yield stresses are much too low to transmit the heavy-duty torques required, and a design to accommodate much larger multiplate coupling areas is not feasible (the corresponding power consumption with current ER fluids would be too high, anyway).

Although the automotive industry is the most likely candidate for large-scale applications of ER fluids, one must also note the increasing involvement of the military industry, particularly in developing ER isolation systems for weapons, radar, and fuel tanks in helicopters and aircraft. Innovative use of ER technology is possible for many other feedback control systems and smart actuators with the most disparate purposes and complexities, such as variable-resistance exercise equipment (e.g., rowing simulators), rheoelectric motors, tracking devices for copying machines, ER clamps to fix workpieces, joints and artificial muscles for robotic arms and prosthetic limbs, penile implants, reconfigurable Braille displays, and so on. ER fluid and solid materials also function in *adaptive structures.* For example, they could be included in high-stress sections as active structural members of bridges, buildings and plants, to control and damp their dynamic responses to windstorms and earthquakes. Likewise, modulation of stiffness with speed in airfoils, helicopter blades, and hydrofoils could be optimally controlled with ER systems. Still other applications may exploit the effective thermal conductivity or convective heat transfer of ER fluids (which also increase with the magnitude squared of the applied electric field) for heat exchange systems, acoustic properties for designing ER filters, delay lines, and ultrasound finders, and optical properties for color films.

Further reviews of ER fluid applications are provided, for example, in Refs. 42 and 47. Technical papers on ER devices are periodically presented in various ER conferences (23,24,48–54).

FUNCTIONING AND DESIGN OF BASIC ER DEVICES

The functioning and design of basic ER devices are easy to understand, in principle. For example, an ER torque-transmitting device may consist simply of an inner cylindrical rotor mounted on a driving shaft, an outer cylinder coaxial to the rotor and mounted on bearings, and an ER fluid in between. Applying a potential difference between the rotor and the outer cylinder induces the ER effect in the fluid, which thus provides the rotational coupling. To increase the coupling area, the torque-transmitting device may alternatively consist of parallel coaxial (multiplate) disks rotating relatively to one another. See, for instance, Fig. 7 in Ref. 47.

An ER torque-transmitting device that has either coaxial cylinders or rotating disks can function as an automotive clutch. In the former configuration, the car engine is connected to the outer cylinder, and the drive shaft powers the wheels through a reduction gear. The inertia of the outer cylinder hardly matters, given the high inertia of the driving motor, which runs at fairly constant high speed. On the other hand, the inner rotor must have low inertia to provide a fast response. That can be attained by using a lightweight nonmetallic material, coated with a conducting thin film to provide the electrical contact. When solidified, the ER fluid forces the drive shaft to rotate in connection with the engine. When liquified, the ER fluid allows the engine to disengage from the drive shaft and spin freely, as if in neutral gear. The almost instantaneous and continuously variable response of the ER fluid to the applied potential provides a prompter and smoother control than a conventional mechanical clutch. Clearly, the nonslip fluid clutch also has fewer parts to wear or fail.

Attaching the outer cylinder to the car body, the same ER coupling device can function as a brake. Relative motion of the cylinders can be gradually stopped with optimal antilock feedback by rapidly modulating the applied voltage with a computerized control system. Heating must be removed by a cooling circulation system, or stability problems may arise in the ER fluid. More complex electrohydraulic brake actuators can be designed; see, for instance, Fig. 24.7 in Ref. 20.

The same torque-transmitting device may also serve as an ER damper. Keeping the outer cylinder fixed, the torsional vibrations of the inner rotor can be damped out by controlling viscosity changes in the ER fluid. Alternatively, a design more similar to ordinary shock absorbers can be used. An ordinary shock absorber consists of a cylinder with a sliding piston inside, which pumps a viscous oil out of a small orifice when pushed in by an outside impact. The oil absorbs and dissipates the impact energy through its slow viscous flow and flows back more quickly into the cylinder through a large orifice after the shock, when the piston rebounds. However, the oil viscosity changes with temperature, which causes the shock absorber to perform unevenly depending on the weather and the road conditions. Repeated compression on a long bumpy ride may heat up the oil so much that it becomes very thin, and the shock absorber may soften and fail when needed most.

The problem is best addressed by transforming such a passive device into an active one by introducing a fast electromechanical valve, which adaptively adjusts the size of a single orifice in response to the piston movement. Without moving parts, an ER valve provides a simpler and even better solution. The microprocessor that senses the piston motion modulates the applied voltage rapidly, which instantly thickens the ER fluid in midstrokes for maximal damping and thins it again immediately afterward for quickest flow-back. In this fixed-plate valve configuration, the piston forces the ER fluid to flow through a stationary annular duct, and the voltage is applied across this duct. In an alternative sliding-plate configuration, the piston itself acts as the grounded electrode, and the damping force originates from the controlled shear resistance between the piston's cylindrical surface and an adjacent motionless surface, which acts as the other electrode; see Fig. 8 in Ref. 47.

High shear stress (over 5 kPa) at high shear rates of the ER fluid is necessary for optimal functioning of ER shock absorbers. Prototypes have been larger than desirable to accommodate the necessary ER valve surface area. However, newly developed ER dampers within a conventional package size have been recently tested on a Ford Thunderbird and performed better than the standard suspensions of the SC and LX models, at least when operated within the optimal temperature range of the ER fluid (55).

The basic design concept of an ER valve is simply that of an ER fluid flowing through a thin section of a pipe. At zero field, the corresponding low viscosity causes only a small drop in pressure between the beginning and the end of the pipe section (at least at low flow rates). When a potential difference is applied between two sides of the section, the viscosity increases, causing controllable resistance to the flow and a correspondingly large pressure drop. More complex additions of diaphragm seals may permit isolating the ER fluid from other hydraulic fluids.

ER valves of various design can be used in a host of devices and most effectively in engine mounting. In an automobile, that must satisfy two contrasting demands. On the one hand, it must insulate the passenger compartment from engine vibrations and noise, which requires low dynamic vertical stiffness and low damping at high frequencies (~100 Hz), to leave alone as much as possible the engine's small-amplitude forced oscillations. On the other hand, the mounting must protect the engine from jolts caused by the pavement, which requires high stiffness and high damping at the natural low frequency (~10 Hz) of the engine-mount system, to prevent the persistence of large-amplitude excursions transmitted to the engine. Current fluid-filled passive mounts made of rubber and metal partially resolve this contradiction by adopting a two-chamber design. When road shake occurs, the fluid flows back and forth between the chambers through an orifice or a short tube, dimensioned to provide substantial damping only at the troublesome low frequency. With the aid of a fluid decoupler, the mount can be further tuned to suppress two unwanted low frequencies or a narrow frequency range. At high frequencies, fluid inertia in the tube is carefully exploited to reduce the damping flow. However, that cannot be totally prevented and compromises noise isolation.

Such a passive mount can be made active be adjusting damping in response to a sensor of engine motion. This can be achieved by adding a fast electromechanical valve designed to adaptively reduce the orifice at low-frequency jolts, while leaving it large and inactive at high-frequency constant engine vibrations. Such a design works effectively, but the valve mechanism itself adds noise, weight, complexity, and cost to the system. A better solution consists of replacing the hydraulic system (fluid and orifice) of the passive mount with an ER valve separating the two chambers, now filled with an ER fluid; see, for instance, Fig. 6 in Ref. 47. When transiently activated in response to a low-frequency jolt, the ER fluid quickly provides the high viscosity needed to damp it. Then, it immediately returns to zero-field low viscosity, providing good isolation to high-frequency constant engine vibrations (56). Because the ER valve has no moving parts, this allows for a simpler, quieter, less expensive, and faster design. Flow volumes and shear rates are relatively low, and a yield stress of only 1 to 2 kPa is needed for this type of application. Hence, ER fluid-filled engine mounts are already practical and advantageous for commercial use.

Other simple ER devices (ER valve in a reciprocating piston system, safety valve, dielectric suspension pump, pulsating pressure generator, pulverizer, filter, settler) are sketched in Sec. 24.11 of Ref. 20. Illustrated therein are also membrane transducer devices (grinding-polishing tools, peristaltic pump) based on *electrodilatancy,* that is, the ability of certain ER systems to undergo rapid and reversible volumetric expansion in response to an electric field. More detailed descriptions and critical assessments of these and more refined ER applications are provided, for example, in Refs. 44, 47, and 57.

NEWTONIAN FLUIDS AND ELASTIC SOLIDS

The simplest model of a fluid (like water or air) is that of an *isotropic continuous medium.* An *ideal fluid* is further assumed to be *nonviscous,* hence, unable to sustain shear stress under either static or dynamic conditions. Then Newton's second law for a fluid element of mass $dm = \rho(\boldsymbol{x}, t)dV$ is given by

$$\rho \frac{d\boldsymbol{v}}{dt} = \rho \boldsymbol{f} - \nabla P \tag{1}$$

where ρ and $\boldsymbol{v}$ are the element density and velocity, and P and $\boldsymbol{f}$ are the pressure and the applied force per unit mass acting on the fluid element. All of these quantities are func-

tions of position $\boldsymbol{x}$ and time t, viewed as independent variables (Eulerian description). However, d/dt represents the total derivative

$$\frac{d}{dt} = \frac{\partial}{\partial t} + \boldsymbol{v} \cdot \nabla \tag{2}$$

which provides the rate of change following the fluid element in its motion (Lagrangian description).

Conservation of matter independently requires the *continuity equation*

$$\frac{\partial \rho}{\partial t} + \nabla \cdot \boldsymbol{j} = 0 \tag{3}$$

where $\boldsymbol{j} = \rho \boldsymbol{v}$ represents the mass current density.

Conservation of linear momentum implies

$$\frac{\partial}{\partial t}(\rho v_i) = \rho f_i + \sum_{j=1}^{3} \frac{\partial T_{ij}}{\partial x_j} \tag{4}$$

where T_{ij} is the *stress tensor.* For an ideal fluid,

$$T_{ij}^{\mathrm{id}} = -P\delta_{ij} - \rho v_i v_j \tag{5}$$

Note that $\rho v_i v_j$ represents convective transport of momentum (per unit area per unit time) and corresponds to the convective part of Eqs. (1) and (2). In fact, as physically expected, Eq. (1) and Eqs. (4–5) are completely equivalent, if Eq. (3) is satisfied.

The vectorial dynamical Eq. (1) and the scalar continuity Eq. (3) provide four relationships for five unknown functions: $\boldsymbol{v}$, P, and ρ. Thermodynamics may provide an additional equation of state, relating P to ρ and entropy per unit mass in the energy representation, or P to ρ and temperature in the free-energy representation. Nonviscous flow is typically nondissipative, hence, *isentropic,* which leads to an additional equation representing conservation of kinetic plus internal energy. Equivalently, flow at constant entropy allows relating P just to ρ through the thermodynamic equation of state. In principle, this yields a unique solution for all five unknown functions, $\boldsymbol{v}$, P, and ρ, given appropriate boundary conditions. In practice, solution of the hydrodynamic equations (even for ideal fluids) may be very difficult, because of the intrinsic *nonlinearity* in the fluid velocity field, originating from the convective transport of momentum. However, considerable simplification occurs in the special but important case of isentropic *irrotational flow,* which leads to Bernoulli's theorem. Full discussion and detailed derivation of all these standard results are readily found in many textbooks, for example, Chap. 9 of Ref. 58, or Chap. 1 of Ref. 59.

Viscous fluids are much more complicated than ideal fluids because they sustain shear stress under dynamic conditions and involve dissipation. One can still retain Eq. (4) representing momentum conservation, provided that a viscous component is added to the stress tensor. An isotropic classical fluid which obeys a linear relationship, first postulated by Newton, between shear stress and shear rate is called a *Newtonian fluid.* Consider the basic configuration of steady laminar shear flow shown in Fig. 1, where the fluid velocity increases with height. Take a horizontal plane $y = y_0$ of constant flow velocity. The drag force F_x exerted on the fluid below the area element dA is given by

$$F_x = \eta \frac{\partial v_x}{\partial y} dA \tag{6}$$

where η is the *viscosity,* measured in Pa·s [we generally adopt the International System of Units (SI) in this article].

In general, given an area element dA oriented with an outward normal unit vector $\boldsymbol{n}$, the stress tensor is defined as

$$F_i = \sum_{j=1}^{3} T_{ij} n_j dA \tag{7}$$

where F_i are the components of the total force exerted by the outside fluid on dA. Then, in the configuration of Fig. 1,

$$\tau = T_{xy} = \eta \frac{\partial v_x}{\partial y} = \eta \dot{\gamma} \tag{8}$$

where τ is the corresponding *shear stress* component and $\dot{\gamma}$ is the *shear rate* of strain.

Conservation of angular momentum requires that the stress tensor be symmetrical. Assuming that its viscous part T_{ij}^{v} is still linear in the velocity gradients for the most general flow configuration, it follows that

$$T_{ij}^{\mathrm{v}} = \eta \left(\frac{\partial v_i}{\partial x_j} + \frac{\partial v_j}{\partial x_i} - \frac{2}{3}\delta_{ij} \nabla \cdot \boldsymbol{v} \right) + \zeta \delta_{ij} (\nabla \cdot \boldsymbol{v}) \tag{9}$$

where ζ is called the *bulk viscosity.* For *incompressible flow,* $\nabla \cdot \boldsymbol{v} = 0$, and ζ plays no role, whereas for compressible flow, it contributes only to the diagonal compressive-tensile components of the stress tensor.

Introducing the complete stress tensor

$$T_{ij} = T_{ij}^{\mathrm{id}} + T_{ij}^{\mathrm{v}} \tag{10}$$

of a Newtonian viscous fluid into the momentum-conservation Eq. (4), with simple manipulations (again involving the conti-

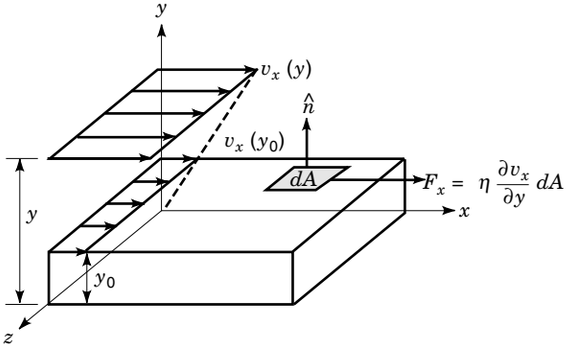

Figure 1. Viscous drag force exerted by the fluid above the $y = y_0$ surface on the fluid below for steady laminar shear flow (58).

nuity equation),

$$\rho\left[\frac{\partial \boldsymbol{v}}{\partial t}+(\boldsymbol{v}\cdot\nabla)\boldsymbol{v}\right]=\rho\boldsymbol{f}-\nabla P+\eta\nabla^2\boldsymbol{v}+\left(\frac{1}{3}\eta+\zeta\right)\nabla(\nabla\cdot\boldsymbol{v}) \quad (11)$$

which clearly reduces to Eq. (1) for an ideal fluid. For incompressible flow, the last term in Eq. (11) vanishes, and the celebrated Navier–Stokes equation is obtained.

Again a unique solution requires an additional energy balance equation, which is more involved than that for a nonviscous fluid. Now there are entropy changes caused by intrinsic viscous dissipation and possibly heat conduction or heat sources in the fluid. A full discussion and derivation of that and of all the basic results for Newtonian viscous fluids can be found, for example, in Chap. 12 of Ref. 58, or in Chap. 2 of Ref. 59.

Unlike an ordinary fluid, an elastic solid can sustain shear stress in a static configuration. Then we have a linear relationship between the stress tensor and the *elastic strain tensor.* In the *isotropic continuum model,*

$$T_{ij}=G\left(\frac{\partial u_i}{\partial x_j}+\frac{\partial u_j}{\partial x_i}-\frac{2}{3}\delta_{ij}\nabla\cdot\boldsymbol{u}\right)+K\delta_{ij}(\nabla\cdot\boldsymbol{u}) \quad (12)$$

where $\boldsymbol{u}$ is the local deformation and G and K are elastic constants, called, respectively, the *modulus of rigidity* and the *bulk modulus.* Because the rate of deformation $\boldsymbol{v}(\boldsymbol{x}, t)$ is $\partial/\partial t\boldsymbol{u}(\boldsymbol{x}, t)$, Eq. (12) for an elastic isotropic solid corresponds to Eq. (9) for a Newtonian viscous fluid. In the shear configuration corresponding to that of Fig. 1 for a viscous fluid, the shear stress τ is related to the *shear strain* component γ by

$$\tau=T_{xy}=G\frac{\partial u_x}{\partial y}=G\gamma \quad (13)$$

which corresponds to Eq. (8) for a viscous fluid. So, G is also called the *shear modulus.*

These observations are all that we need to introduce non-Newtonian fluids, which often exhibit properties hybrid between solids and liquids. A more adequate treatment of elastic continua can be found, for example, in Chap. 13 of Ref. 58, or in Ref. 60.

NON-NEWTONIAN FLUIDS

Despite their fundamental and practical importance, Newtonian fluids represent only a small class of all substances that flow under certain conditions (as opposed to solids). For all such substances, one may still define an apparent viscosity as the ratio between shear stress and shear rate, but that varies typically with shear rate. For instance, the apparent viscosity may be large or even infinite at a low or vanishing shear rate, but rapidly decreasing at higher shear rates. Common substances, such as yogurt, mayonnaise, white of egg, condensed milk, toothpaste, shampoo, foams, and chewing gum, display such behavior, called *shear-thinning:* they hardly flow under their own weight but flow readily when squeezed. Other substances do the opposite, becoming more viscous rather than less viscous at larger shear rates. This behavior, called *shear thickening,* can be simply demonstrated by mixing powdered cornstarch with water in a glass. The suspension easily flows and pours like whipping cream if the glass is tilted slowly. However, it immediately hardens upon stirring or shaking. Furthermore, once hardened, the paste occupies a larger volume, looks drier, and returns to its initial condition only slowly. The combination of these effects is variously called dilatancy, rheopexy, or antithixotropy. Its opposite, namely, a shear-thinning substance that recovers its full rigidity only long after shearing has stopped, is called *thixotropic.* Bentonite gel is a classical example. Thixotropy makes paint easier to apply and mud easier to drill.

Various suspensions and polymeric liquids often exhibit both shear-thinning and shear-thickening behavior. Shear thinning occurs at modest shear rates, followed abruptly by shear thickening at greater shear rates. In general, any material that obeys an essentially nonlinear *constitutive relation* between shear stress and shear rate is called a *non-Newtonian fluid.* Liquids that obey quantum mechanical, rather than classical laws, such as liquid helium, are also called non-Newtonian: we are not concerned with such systems at all in this article. Non-Newtonian fluids may be anisotropic and obey tensorial constitutive relations, requiring definition of several (shear-rate dependent) viscosity coefficients. Typically, non-Newtonian fluids possess long relaxation times, compared to the inverse of the velocity gradients that can be applied. Hence, constitutive relations may not depend only on the instantaneous shear rate but rather on its integration over the specimen's history. Thixotropy obviously depends on that. Actually, for most non-Newtonian fluids, constitutive relations are unknown, depend on other poorly defined functions, or are too empirical and particular to provide much insight. In any such case, real progress in understanding can be made only through microscopic investigation or simulation of the structure and properties of the particular system under consideration.

The range and study of non-Newtonian fluids is vast and complex and occupies most of modern rheology. In the following, we only consider a few basic aspects regarding ER suspensions. Further background in this important and fascinating field can be obtained, for example, from Refs. 61–63.

ER FLUID RHEOLOGY

Most ER suspensions behave essentially as Newtonian fluids in the absence of any applied electric field. Their viscosity is only a few times larger than that of the dispersant fluid and is adequately described by relatively simple models and equations. In fact, the viscosity of a low-concentration suspension of N spherical particles of radius a in a volume V was first calculated by Einstein in 1906. It is just the viscosity of the dispersant times $(1 + 2.5v)$, where $v = 4\pi Na^3/3V$ is the volume fraction of the spheres; see Sec. 22, Chap. 2, of Ref. 59. Appropriate generalizations for higher concentrations and/or nonspherical particles are reported, for example, in Refs. 62 and 64.

When an electric field is applied, the overall behavior of most ER fluids resembles that of a field-induced shear-thinning *Bingham plastic.* The corresponding constitutive relation is

$$\tau(E)=\tau_y(E)+\eta_\infty\dot{\gamma} \quad (14)$$

where $\tau_y(E)$ is the yield stress, essentially proportional to the electric field's magnitude squared, and η_∞ is called the high-shear limiting or *plastic viscosity*. In this basic model, η_∞ is constant (at any given temperature) and coincides with the *differential viscosity* $d\tau/d\dot{\gamma}$. The plastic viscosity also coincides with the *zero-field viscosity*. Typically, both the yield stress and the zero-field viscosity increase with particle concentration, which determines an optimal concentration to maximize the ER effect and minimize the zero-field viscosity for any specific application. On the other hand, the effective or *apparent viscosity*

$$\eta(E, \dot{\gamma}) = \frac{\tau(E)}{\dot{\gamma}} = \frac{\tau_y(E)}{\dot{\gamma}} + \eta_\infty \tag{15}$$

depends on both the electric field and the shear rate. It diverges at low shear rate (for nonzero field), and approaches η_∞ at high shear rates. The parallel lines A and B in Fig. 2 represent Eq. (14) at nonzero and zero field, respectively.

A more accurate description of ER behavior requires considerable corrections to the basic Bingham plastic model, particularly at low shear rates. A typical situation is shown as curve C in Fig. 2. Applying an electric field at zero shear rate, a viscoelastic solid forms. The corresponding *static yield stress* $\tau_{sy}(E)$ is defined operatively as the shear stress necessary to initiate flow from solid state equilibrium, regardless of whether the Bingham plastic model fits the ER fluid behavior at later shearing conditions. After $\tau_{sy}(E)$ is applied and flow is established, the shear stress immediately drops with increasing shear rate and quickly approaches curve A predicted by Eq. (14). Having attained that, if the shear rate is reversed all the way back to zero, the shear stress remains close to curve A. Therefore, $\tau_y(E)$ is called the Bingham or *dynamic yield stress* and is defined as the zero-shear-rate intercept of the linear Bingham plastic model, which generally provides a good fit at sufficiently high shear rates. Now, it takes only a short time before $\tau_{sy}(E)$ is fully recovered under static conditions. Hence, thixotropy is usually limited (barring structural alterations after prolonged shearing). However, what causes the usually positive difference between the static and the dynamic yield stress, an effect called stiction, is not well established.

Further deviations and complications may occur. For example, the plastic viscosity may depend to some extent on the shear rate (typically shear thinning). Inclusion of this dependence in Eq. (14) generalizes the Bingham model to that of a *viscoplastic fluid*. The Herschel-Bulkley model is a particular case, which adds an exponent n to $\dot{\gamma}$ (and renames its coefficient) in Eq. (14). The defining feature of all such models remains the presence of a finite dynamic yield stress. On the other hand, the static yield stress may turn out to be smaller than that, or it may even vanish at low fields; see curve D in Fig. 2. Furthermore, the dependence of either static or dynamic yield stress on the applied electric field often deviates from precisely quadratic, most noticeably at high fields.

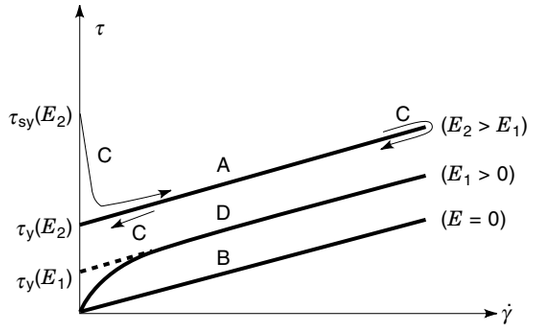

Figure 2. Shear stress vs. shear rate. Curve A: Bingham plastic model (nonzero field). Curve B: zero-field Newtonian fluid. Curve C: typical ER behavior. Curve D: pseudoplastic behavior.

The Bingham plastic and related models are reasonably appropriate only in the *post-yield regime,* where flow is established. That is, of course, essential to most ER applications, which involve dynamic conditions and require knowledge of the corresponding shear strength. However, the *pre-yield regime* is also important, for example, in designing nonflowing devices, such as seals and safety valves, where the fluid is expected to remain solidified below a certain pressure threshold, or in flexible and adaptive structures, which must provide a controllable mechanical response or vibration damping without continuous alteration (47). In such a regime, the assumption of total rigidity as in the Bingham plastic model is obviously inadequate. Instead, we must at least consider an elastic relationship such as that of Eq. (13), for shear stress below yield and for shear strain below a corresponding *yield strain*. The next step necessary is to consider a *viscoelastic model* (62), which assumes a linear relationship between shear stress and both shear strain and its shear rate:

$$\tau = G\gamma + \eta\dot{\gamma} \tag{16}$$

Applying an oscillating shear strain of small amplitude and sinusoidal time dependence $e^{i\omega t}$, we can transform Eq. (16) into

$$\tau = G\gamma + i\omega\eta\gamma = G^*(E, \omega)\gamma \tag{17}$$

which again resembles Eq. (13). Now, however, G^* is a complex shear modulus, whose real part G', called *storage modulus,* provides the coefficient for stored elastic energy (quadratic in strain) and whose imaginary part G'', called *loss modulus,* accounts for viscous energy loss and relaxation. Study of the dependence on both the applied electric field E and the frequency of shearing ω for both G' and G'' provides important information about the structure and properties of the ER solidified suspension in the pre-yield regime (15,27,65–67).

The transition from the pre-yield to the post-yield regime involves larger strain amplitudes, hence, nonlinear relationships and a more complex Fourier analysis, whose precise interpretation and connection with experimental observations in such a *yield regime* is more difficult to establish.

For simplicity, the discussion in this section has been limited to one-dimensional shearing. However, many ER applications involve more complex three-dimensional flows. Then appropriate tensorial generalizations of models and equations such as Eqs. (14)–(17) are required. These are relatively easy to obtain, but they cannot always be uniquely determined from purely theoretical principles. More serious difficulties occur if one abandons the common assumption of a symmetrical stress tensor, which is not quite justified in the presence of an electric field. That makes the ER fluid inherently anisotropic.

Further complications arise when the flow or the electric field change along a streamline. These are called *extensional deformations* and occur, for example, in an ER valve of varying cross section. These issues are subjects of current and future research (27, 68).

A further review of phenomenological models and comparison with experiments is provided in Refs. 6, 43 (see their Figs. 1–2, in particular) and Ref. 64.

ER FLUID RHEOMETRY

There are many techniques for measuring ER properties. Some are more suitable for general material characterization, and others are more focused on potential end uses. The two basic operating modes of ER devices define two broad classes of electrode configurations used to test ER materials.

The first class comprises sliding-plate instruments, involving either parallel plates or coaxial cylinders. Parallel plates may be (circular and) rotating or (rectangular and) translating relative to each other. Coaxial cylinders may be rotating (Couette configuration) or axially sliding relative to each other. Rotational geometries are necessary for continuous (steady state) shear measurements and are generally easier to implement. Among them, coaxial cylinders with a narrow gap (compared to their radii) have the advantage of providing a nearly constant (radially) shear rate, whereas rotating parallel disks generate a shear rate increasing linearly with distance from the axis, which makes a rigorous interpretation of the data more difficult. Moving electrodes are electrically grounded with a carbon brush, a copper/beryllium spring, or a running contact via a conducting fluid (e.g., mercury). Cone-and-plate viscometers, commonly used in other rheological measurements, are not suitable for ER fluids, because they involve largely nonuniform electric fields, especially around the cone apex.

The operating modes of sliding-plate instruments involve either a controlled stress or a controlled shear rate. For example, in a Couette-type rheometer, stress is controlled by attaching the inner cylinder to a motor, while keeping the outer cylinder fixed. The motor supplies a given torque, and the angular velocity Ω that results in the inner cylinder is measured. For a Newtonian fluid, the viscosity is given by

$$\eta = \frac{\tau}{\dot{\gamma}} = -\tau \frac{R_2^2 - R_1^2}{2R_2^2\Omega} \approx -\tau \frac{R_2 - R_1}{R_2\Omega} \tag{18}$$

where R_1 and R_2 are the radii of the inner and outer cylinders, $(-\tau\, R_1)$ is the positive (counterclockwise) torque exerted by the inner cylinder on the fluid per unit area, and $\dot{\gamma}$ is the (negative) shear rate at R_1. This result is easily derived by solving the Navier–Stokes equation with no-slip boundary conditions at the cylinders; see, for example, Sec. 18, Chap. 2, of Ref. 59. The last approximate expression in Eq. (18) applies for $R_2 - R_1 \ll R_1$. In this case, the shear rate hardly falls radially, and the expression is also approximately valid for the apparent viscosity of a Bingham plastic, provided that the yield stress is exceeded all the way to the outer cylinder (61,64).

Conversely, the shear rate is controlled by rotating one cylinder at a given angular velocity and attaching the other cylinder to a calibrated spring, whose deflection measures the torque transmitted through the fluid (which is equal and opposite to the torque that must have been applied to the driving cylinder to keep it at the given angular velocity). The choice of driving the outer cylinder in the shear-rate controlled operating mode is often preferred for flow stability. In general, shear-rate controlled rheometers maintain flow stability at higher torques and shear rates, thus allowing better extrapolation of large dynamic yield stresses from low high-shear-limiting viscosities, as desired in ER applications.

Post-yield measurements are typically conducted in continuous. Full investigation of pre-yield and yield regimes requires various other conditions. The static yield stress is conveniently determined by stress-controlled rheometers by gradually increasing the torque from an initially static configuration until flow onset. On the other hand, full determination of the viscoelastic response requires further measurements conducted with constant strain, oscillatory strain at various frequencies and amplitudes, and sudden application of shear strain or shear rate.

The second class of electrode configurations involves forced flow through fixed plates, as in ER valve applications. The fixed plates to which the potential difference is applied may be plane and parallel, as in slit or rectangular ducts, or they may be coaxial cylinders, as in annular channels. Capillary rheometers are not suitable for ER measurements, because they can hardly be configured as electrodes providing uniform fields.

These instruments typically measure the pressure gradient for steady flow. The pressure gradient equals the yield stress divided by an appropriate fraction of the electrode gap (see, for instance, Eq. (4) of Ref. 47 for the basic slit configuration). Assuming Bingham plastic behavior (see, for instance, Chap. 3 of Ref. 61), the complete velocity profile in the channel can also be calculated. Solidification of the ER fluid starts around the pipe center, where shear is lowest, and proceeds outward with increasing electric field until a complete shut-off of the valve occurs. The total pressure drop between the inlet and outlet of the valve is proportional to both the yield stress and the length of the valve and can be as high as 6.9 MPa (1000 psi) (47).

At zero field, all types of measurements typically give consistent results for the essentially Newtonian dispersions. Unfortunately, that is not necessarily the case when the electric field is applied because that makes ER suspensions inherently anisotropic, and some observations become dependent on the geometry. Even within the same geometry, such as flow through a rectangular duct, measurements of the apparent viscosity may differ, depending on the duct gap. In fact, a first-order theoretical analysis suggests a decrease in apparent viscosity at large gaps as a result of ER fluid anisotropy (68). Fortunately, at least the static yield stress is not affected and corresponding measurements are reasonably consistent and independent of the geometry.

Further discussions and review of rheometric characterizations and testing of ER fluids can be found, for example, in Refs. 6,47,64.

THEORETICAL MODELS AND SIMULATIONS OF ER PHENOMENA

Electrical interactions are clearly at the origin of the ER effect. When an electric field is applied, the particles polarize

and in turn generate nonuniform fields. In such fields, polarized particles, although neutral, migrate toward regions of higher field intensity, an effect called *dielectrophoresis* (69). Such regions are closer to other particles, which leads to further polarization, attraction, and aggregation. Ultimately, the strong polar interactions produce fibrous structures preferentially aligned with the applied field. In diluted suspensions, particles may have to travel over considerable distances. In weak applied fields, their movement may be slow. Hence, the response time for fibrillation may be considerable. However, for typical ER concentrated suspensions in strong applied fields, particles need to move a distance only a fraction of their size to form fibrous structures, and a fast (millisecond) response can occur. The subsequent evolution and reaction of the fibrous structures under static and dynamic shearing conditions (aggregating, stretching, tilting, breaking, and reforming) are ultimately responsible for all of the observed ER phenomena. Such evolution is continually determined by the balance of the microscopic electric and hydrodynamic forces acting on the particles.

There is a relatively general agreement about this basic scenario of fibrillation induced by polarization, which was first envisioned by Winslow himself (2). However, which specific mechanisms are responsible for particle polarization in various types of ER fluids has not yet been fully established. Some models involve electrical double layers typically produced by ions in water surrounding the particles. Other models focus on the interfacial polarization resulting from the difference in permittivities between the particles and the dispersing medium. These two types of models may be equivalent in some instances, for example, for thin double layers and particles with thin coatings, or they may be essentially incompatible, for example, for double layers presumed to act through large distortions and overlap. In any event, the ER activity is controlled much more by interfacial effects than dielectric bulk properties of the particles. A more detailed and precise understanding of the microscopic structures and phenomena occurring at the particle surfaces is required for intelligent selection and development of more effective ER fluid components. In parallel with the uncertainties in characterization and microscopic description of electrical interfacial properties and partly as a result of those uncertainties, there is no definitive account of how fibrillation develops and evolves under shear, what relaxation times are involved at various stages, and various other dynamical characteristics. More detailed discussions and references on various proposed models and mechanisms for the ER effect can be found, for instance, in Refs. 6, 18, 19, 27, and 70.

A complete and truly predictive theoretical account of ER phenomena must satisfy two essential requirements. The first is the proper and quantitative treatment of the underlying electrical interactions. The second requirement is the modeling and simulation of the fibrous structure statics and dynamics based on the adequate treatment of both electric and hydrodynamic forces.

With regard to the first requirement, three crucial features must be considered. First, the electrical interactions in ER fluids are inherently *multipolar* and *multiparticle.* Because particles are in contact or very close to one another, the electric field that they contribute is very complicated and varies rapidly on the scale of the particle dimensions. The great strength of the resulting electrical interactions derives from many multipolar terms. A purely dipolar system is an inadequate model, which cannot consistently provide correct results for actual fluids with an ER effect strong enough to be of practical interest. For those, the higher multipolar terms provide a much stronger contribution than just the dipolar interactions, exhibit a quite different and more complex angular dependence, and decrease much faster with the distance between the particles. Likewise, pair interactions alone cannot provide a realistic description of the self-consistent polarization cooperatively induced by many particles at close range.

Secondly, ER fluids operate between electrodes. The basic electrode configuration can be regarded as a parallel-plate capacitor (PPC), because the radius of curvature of the electrodes is typically much greater than their separation. Theoretically, the PPC configuration can be treated by considering *image multipoles* of the particles. The reflection of one particle on the right (or left) electrode results in one image, but the reflection of this image on the left (or right) electrode results in a new image further away, which in turn reflects on the right (or left) electrode, and so on. Hence, each particle generates an infinite set of images. The electrical interaction between a particle and the electrodes equals that between the particle and all of its images, as well as the images of all the other particles. The image multipoles are not equal to those of the real particles, although they are related [see Eq. (26) later]. Hence, the system cannot be equivalently described by an infinite system, consisting only of real particles immersed in a uniform external field (UEF), somehow produced by fixed external charges. Basic ER properties, such as yield stress and apparent viscosity, crucially depend on regions where the weakest electrical interactions occur, because particle chains typically break there first. Therefore, it is necessary to find out whether these regions occur near the electrodes or in the bulk, depending on the system and the static or dynamic shearing configuration (15,18,19,70). The UEF configuration may provide results equivalent to the PPC configuration in the bulk, but it cannot account for exact particle interactions near or with the electrodes. In fact, surface effects cannot be calculated ignoring the image multipoles, because their contributions near the electrodes are different but just as important as those of the particles.

Thirdly, real particles in ER fluids cannot be treated as uniform spheres because they typically have a nonuniform electrical response and a complex structure, which required both to augment the ER effect and to stabilize the fluid (recall, for example, the corresponding roles played by activators and surfactants). A uniform electric field induces only a dipole moment on a spherical particle. In that case, the usual polarizability, which is the ratio between the induced dipole moment and the uniform electric field, is sufficient to describe the electrical response of the particle. However, a multipolar electric field induces multipolar moments on any particle (even on a simple homogeneous sphere). Therefore, to begin with, a realistic description of ER fluids requires determining the complete electrical response of isolated complex particles to any field. This involves *generalized polarization coefficients,* defined as the tensorial ratio between a multipole of given order induced on the particle and the inducing multipolar field component of any other order.

These complexities in electrical interactions have limited most theoretical models and simulations of ER phenomena

largely to dipolar approximations. As a result, even though those models and simulations may suggest real effects in some respects, none can be regarded as conclusive, nor is there any rigorous way to select one model over another. However, full treatments of multipolar interactions have been progressively developed (71–76), and a complete theory and computational scheme of electrical interactions in ER fluids, which includes all three crucial features just mentioned, has recently become available (75–76). Therefore, the first essential requirement for a truly predictive theoretical account of ER phenomena has in fact been fulfilled, even though the second still has not.

The widespread use of dipole approximations also results from the fact that, occasionally, dipolar estimates are sufficient to suggest trends roughly agreeing with observation. For example, consider a uniform sphere of radius a and dielectric constant ϵ_p in a host medium of dielectric constant ϵ_h. A uniform electric field $\boldsymbol{E}$ acting on the particle induces a dipole moment (see, for example, Sec. 4.4 in Ref. 77)

$$\boldsymbol{p} \propto \beta a^3 \boldsymbol{E} \tag{19}$$

where

$$\beta = \frac{\epsilon_p - \epsilon_h}{\epsilon_p + 2\epsilon_h} \tag{20}$$

If two particles with such induced dipole moments interact, the corresponding force between them is proportional to p^2/a^4 at contact. Then, the yield stress scales as

$$\tau_y(E) \propto \beta^2 E^2 v \tag{21}$$

where v is the volume fraction of the particles in the fluid. Quadratic dependence on the electric field of the yield stress is basically confirmed by observations. However, we show in the next section that in a complete theory of electrical interactions this is just a consequence of linear response in a fixed or steady-state configuration, regardless of any dipolar model or approximation. Equation (21) further suggests a linear dependence of the yield stress only on the volume fraction of the particles, not on their absolute size. This is also confirmed by experiment, at least for particles not so small (in the submicron range) that Brownian motion effectively reduces the yield stress.

Introducing the yield stress scaling in the Bingham plastic model, the apparent viscosity may behave as

$$\eta = \frac{\tau_y(E)}{\dot{\gamma}} + \eta_\infty \sim \eta_\infty \left(\frac{\epsilon_0 \epsilon_h v \beta^2 E^2}{\eta_\infty \dot{\gamma}} + 1 \right) \tag{22}$$

suggesting an approximate dependence of the apparent viscosity on the so-called Mason number, defined as

$$M_n = \frac{\eta_h \dot{\gamma}}{2\epsilon_0 \epsilon_h \beta^2 E^2} \tag{23}$$

where η_h is the viscosity of the suspending host medium. Evidently, the Mason number represents the ratio between the order of the hydrodynamic viscous forces microscopically exerted by the dispersant on the particles and the order of the electrical forces between the particles. Then,

$$\eta \sim \eta_\infty \left(\frac{\kappa v}{M_n} + 1 \right) \tag{24}$$

where $\kappa \sim 0.5$ is a system-specific parameter. This scaling relationship agrees fairly well with observations in a rather wide range of fields and shear rates for any given system (64, 78).

Encouraged by the apparent success of these and other simple dipolar estimates, several dipolar models and simulations have been developed to provide microscopic descriptions of ER phenomena. Despite their ingenuity and value in suggesting the possiblity of various mechanisms, none of these models or results can be regarded (nor has been claimed) as conclusive. The limiting factor essentially derives from the underlying dipolar approximations, which at the very least forbid any rigorous or truly quantitative prediction.

Given the power available for current computation, now it is feasible to fully implement the rigorous treatment of the electrical interactions in similar molecular dynamics and Monte Carlo simulations. Accurate inclusion of all significant hydrodynamic forces is also possible. Therefore, a "second generation" of truly predictive simulations and microscopic descriptions of ER phenomena fully satisfying both essential requirements described previously is expected. This may finally provide a complete theoretical understanding of the underlying mechanism of the ER effect, which has been recommended by the DOE expert panel as a critical research need to guide the development of new ER materials and devices (42). Thus we refer, for example, to Refs. 6, 18, 19, and 78–80 for reviews of "first generation" models and simulations, and in the last section of this article we focus on the foundations and some key technical elements of the exact theory of electrical interactions in ER fluids, which is already well established.

THEORY AND COMPUTATION OF ELECTRICAL INTERACTIONS IN ER FLUIDS

The electrical response and activity of an ER fluid is ultimately determined by the microscopic structure and the complex dielectric functions of all of the fluid components, namely, the host liquid and the composite particles, including all sorts of coating layers. In turn, these complex dielectric functions result from the contributions of all mobile charges. Hence, they are generally frequency-dependent, and so is the resulting ER activity. The imaginary part of a complex dielectric function, associated with the conductivity of a particular component, may be dominant. Microscopically, that may be produced by light electrons, or by mobile ions at low frequencies. It is generally advantageous to have those components at or near the particle interfaces to enhance the electrical interactions and the resulting ER effect.

The precise characterization of the microscopic structure and the complex dielectric functions of all of the fluid components may be difficult in practice, but is clearly required for any quantitative modeling and understanding of ER phenomena. Thus, a complete theory of ER fluids must consider particles of arbitrary structures, immersed in a dispersant host medium of dielectric function ϵ_h, filling the space between two

parallel electrode plates at a constant potential difference V_0, and located at $z = -d/2$ and $z = d/2$, respectively.

Let us denote the position of the nth particle by $\boldsymbol{r}_n$, and the multipole moments (with respect to $\boldsymbol{r}_n$) by q_{nlm}. The position of the kth image, resulting from the kth reflection on the right ($k = 1, 2, 3, \ldots$) or left ($k = -1, -2, -3, \ldots$) electrode, is given by

$$\bar{\boldsymbol{r}}_{nk} = \{\bar{x}_{nk}, \bar{y}_{nk}, \bar{z}_{nk}\} = \{x_n, y_n, kd + (-1)^k z_n\} \tag{25}$$

The corresponding image multipole moments are given by [see Eq. (10) of Ref. 81]

$$\bar{q}_{nlmk} = (-1)^{(l+m+1)k} q_{nlm} \tag{26}$$

Obviously, for $k = 0$, $\bar{\boldsymbol{r}}_{n0} = \boldsymbol{r}_n$ and $\bar{q}_{nlm0} = q_{nlm}$ correspond to the particles themselves.

The local electric potential acting on the nth particle is given by [see Eqs. (14) and (15) of Ref. 81]

$$\begin{aligned} U_n^{\text{local}}(\boldsymbol{r}) &= -\sqrt{\frac{4\pi}{3}} E_0 |\boldsymbol{r} - \boldsymbol{r}_n| Y_{1,0}(\boldsymbol{r} - \boldsymbol{r}_n) \\ &\quad + \frac{1}{\epsilon_0} \sum_{l_1 m_1} |\boldsymbol{r} - \boldsymbol{r}_n|^{l_1} Y_{l_1,m_1}(\boldsymbol{r} - \boldsymbol{r}_n) \\ &\quad \times \left[\sum_{n_2 l_2 m_2} \sum_k A_{l_1,m_1}^{l_2,m_2}(\boldsymbol{r}_{n_2 k} - \boldsymbol{r}_n)(-1)^{(l_2+m_2+1)k} q_{n_2 l_2 m_2} \right] \\ &\equiv -\sqrt{\frac{4\pi}{3}} \sum_{l_1 m_1} E_{l_1 m_1} |\boldsymbol{r} - \boldsymbol{r}_n|^{l_1} Y_{l_1,m_1}(\boldsymbol{r} - \boldsymbol{r}_n) \end{aligned} \tag{27}$$

where the coupling coefficients are

$$A_{l,m}^{l',m'}(\boldsymbol{r} - \boldsymbol{r}') = \begin{cases} [A_{l,m}^{l',m'}] \dfrac{Y_{l+l',m-m'}^*(\boldsymbol{r} - \boldsymbol{r}')}{|\boldsymbol{r} - \boldsymbol{r}'|^{(l+l'+1)}}, & (\boldsymbol{r} \neq \boldsymbol{r}') \\ 0, & (\boldsymbol{r} = \boldsymbol{r}') \end{cases} \tag{28}$$

In Eqs. (27) and (28), $Y_{l,m}(\mathbf{r})$ are spherical harmonics, and

$$\begin{aligned} [A_{l,m}^{l',m'}] = &(-1)^{(l'+m')} \left[\frac{4\pi}{(2l+1)(2l'+1)(2l+2l'+1)} \right]^{1/2} \\ &\times \left[\frac{(l+l'+m-m')!(l+l'-m+m')!}{(l+m)!(l-m)!(l'+m')!(l'-m')!} \right]^{1/2} \end{aligned} \tag{29}$$

are numerical coefficients. There are clearly three contributions to the local potential in Eq. (27) that derive from the applied field $E_0 = V_0/d$, the field produced by all of the other particles, and the field produced by all the images (including those of the nth particle under consideration). All orders of multipole moments ($l = 1, 2, \ldots, m = 0, \pm 1, \ldots, \pm l$) are included.

The nth particle may have an arbitrary shape or structure, but if its electrical response is linear (within the range of the applied field), the multipole moments induced on such a particle must be a linear combination of the multipolar components $E_{l_1 m_1}$ of the local potential, namely,

$$q_{nlm} = \sqrt{12\pi}\epsilon_0 \sum_{l_1 m_1} \lambda_{nlm}^{l_1 m_1} E_{l_1 m_1} \tag{30}$$

These equations provide the general definition of the *linear polarization coefficients* (82), that is,

$$\lambda_{nlm}^{l_1 m_1} = \frac{1}{\sqrt{12\pi}\epsilon_0} \left. \frac{\partial q_{nlm}}{\partial E_{l_1 m_1}} \right|_0 \tag{31}$$

where $|_0$ means that the derivatives are evaluated at $E_{l_1 m_1} = 0$, for all l_1, m_1. These polarization coefficients are generalizations of the usual (dipolar) polarizability and depend on the structure and orientation of the particle. Symmetries therein may restrict the number of terms contributing to Eq. (30). For example, spherical symmetry requires a diagonal response, that is, only terms with $l_1 = l$ and $m_1 = m$ may not vanish (see, for example, Eq. (42) for coated spherical particles). For nonlinear particles, additional (and more complex) *nonlinear polarization coefficients* must be similarly introduced (83).

From Eq. (27) for the local potential and Eqs. (30)–(31) defining the polarization coefficients, we obtain a self-consistent set of linear equations for all of the multipole moments:

$$\begin{aligned} q_{nlm} + 3 &\sum_{n_1 l_1 m_1} q_{n_1 l_1 m_1} \\ &\times \left[\sum_{l_2 m_2} \lambda_{nlm}^{l_2 m_2} \sum_k (-1)^{(l_1+m_1+1)k} A_{l_2,m_2}^{l_1,m_1}(\boldsymbol{r}_{n_1 k} - \boldsymbol{r}_n) \right] \\ &= \sqrt{12\pi}\epsilon_0 \lambda_{nlm}^{10} E_0 \end{aligned} \tag{32}$$

This shows that the electrical response is completely and uniquely determined by the polarization coefficients of the particles and the microscopic configuration of the system (determined by the positions and orientations of all the particles). In principle, the set of linear equations for all of the multipole moments is infinite. In practice, the results are well behaved and converge at finite orders of images (k_0) and multipole moments (l_0), although l_0 is typically large for particles at close range. Diverging exceptions occur at most for extreme cases of infinitely conducting and perfectly touching particles, where classical theory itself becomes inadequate. This is not a problem in practice because highly conducting particles must be insulated with thin coatings, to prevent charge transfer between them at contact and to avoid a corresponding large conduction through the ER fluid (29–32).

Now let us consider the total electrostatic energy stored in the system, which is given by [see, for example, Eq. (4.83) of Ref. 77]:

$$W = \frac{1}{2} \int_V \rho_f(\boldsymbol{r}') U(\boldsymbol{r}') dV' \tag{33}$$

where V, $\rho_f(\boldsymbol{r})$, and $U(\boldsymbol{r})$ are the volume, free charge density, and electric potential of the system, respectively. The contribution from the right electrode plate (at $z = d/2$) vanishes because $U_{z=d/2} = 0$. From now on let us assume that the host medium is nonconducting (further consideration of a conducting medium can be found in Ref. 76). Then, the contribution from inside the system also vanishes, because there is no free charge density in either the medium or nonconducting particles, and there is no net free charge on equipotential surfaces of conducting (neutral) particles. Hence, the only contribution to Eq. (33) derives from the left electrode plate and amounts to the free charge Q_f on the electrode plate times V_0. Q_f in-

cludes two parts, one from the applied potential and the other induced by the particles. Using a standard result [see, for example, problem 1.13, p. 51, of Ref. 77],

$$Q_{\mathrm{f}} = \epsilon_0 \epsilon_{\mathrm{h}} \frac{V}{d} E_0 + \frac{\epsilon_{\mathrm{h}}}{d} \sum_n p_{\mathrm{nz}} \tag{34}$$

where $p_{\mathrm{nz}} = \sqrt{4\pi/3} q_{\mathrm{n10}}$ is the z-component of the dipole moment in Cartesian coordinates. Hence,

$$W = \frac{V}{2} \epsilon_0 \epsilon_{\mathrm{h}} E_0^2 + \frac{1}{2} \epsilon_{\mathrm{h}} E_0 \sum_n p_{\mathrm{nz}} \tag{35}$$

The first term in Eq. (35) is the same constant that we have when the medium alone fills the capacitor, and the second term derives from the particles (including their interfacial polarization with the medium).

When the positions and orientations of the particles change, the induced dipole moments change. That in turn produces a change in Eq. (34), corresponding to a charge transfer between the two electrodes. Then, the work done by the electrical source (battery) in response to a change in the microscopic configuration is given by

$$\Delta W_b = V_0 \Delta Q_f = \epsilon_{\mathrm{h}} E_0 \Delta \left(\sum_n p_{nz} \right)_{V_0} \tag{36}$$

where the subscript V_0 indicates that change must be done while keeping the potential difference between the electrodes constant. Subtracting Eq. (36) from the change in Eq. (35), we obtain the work mechanically done on the system to change its configuration:

$$\Delta \mathscr{E} = -\frac{1}{2} \epsilon_{\mathrm{h}} E_0 \Delta \left(\sum_n p_{nz} \right)_{V_0} \tag{37}$$

From this, we can define the *interaction energy* as

$$\mathscr{E} = -\frac{1}{2} \epsilon_{\mathrm{h}} E_0 \sum_n p_{nz} \tag{38}$$

Then, the total electrostatic force exerted by the system (including the effect of the battery) associated with the displacement of a generalized coordinate ξ is given by

$$\mathscr{F}_\xi = -\left(\frac{\partial \mathscr{E}}{\partial \xi} \right)_{V_0} = \frac{1}{2} \epsilon_{\mathrm{h}} \frac{\partial}{\partial \xi} \left(E_0 \sum_n p_{nz} \right)_{V_0} \tag{39}$$

These equations allow us to compute the exact electrostatic interactions in ER fluids. For instance, if we need to compute the electrostatic force on any given particle, we take ξ as a coordinate of that particle, or $\partial/\partial\xi \to \nabla_n$, and

$$\boldsymbol{f}_n = -\nabla_n (\mathscr{E})_{V_0} = \frac{1}{2} \epsilon_{\mathrm{h}} \nabla_n \left(E_0 \sum_n p_{nz} \right)_{V_0} \tag{40}$$

On the other hand, if we wish to compute the shear stress, we take ξ as the angle θ for tilting parallel chains times the system volume:

$$\tau_{\mathrm{y}} = -\left(\frac{\partial \mathscr{E}}{\partial (V\theta)} \right)_{V_0} = \frac{1}{2V} \epsilon_{\mathrm{h}} \frac{\partial}{\partial \theta} \left(E_0 \sum_n p_{nz} \right)_{V_0} \tag{41}$$

Its maximum, varying θ, provides the yield stress. Clearly, the results depend on the system configuration. A few other specific examples are provided later.

The previous equations indicate the evolution of the system from an initially disordered configuration when a potential difference is suddenly applied. Driven by the electrical source, the system undergoes a continuous change until it reaches a microscopic configuration of maximum total dipole moment (hence, polarization). The total electrostatic energy W is maximized, and the interaction energy $\mathscr{E}$ is minimized. The work done by the electrical source splits equally into mechanical work done by the system (negative of the interaction energy change) and total electrostatic energy stored in the system. Thus, the ground state of the solidified ER fluid has maximum total dipole moment and total electrostatic energy and minimum interaction energy. We may note that in the uniform external field (UEF) configuration, the electrostatic energy formally coincides with Eq. (38) (see, for example, Eq. (4.94) and Sec. 4.7 of Ref. 77) and is minimized in the ground state. Then results equivalent to those of the parallel plate capacitor (PPC) configuration may be obtained for forces in the bulk, formally corresponding to a Legendre transformation (84). On the other hand, of course, no surface effect can be properly treated in the UEF configuration.

An important fact shown by Eq. (39) is that forces do not depend on the absolute values of dipole moments in a certain configuration but only on the variations of such dipole moments when the configuration changes (virtually and infinitesimally). This shows that the ER effect is purely a *local field effect.* It is caused by the change induced on the local field acting on each particle by a virtual variation of microscopic configuration. That changes the polarization of the particles, hence, the interaction energy. The *fixed-dipole approximation* considers forces between dipole moments induced on the particles only by a constant (applied) field without any regard for local field changes. That approximation is unrelated even in principle to the real ER effect.

Furthermore, it important to note that although Eqs. (34)–(41) depend explicitly only on dipole moments, these must in turn be determined with Eq. (32), that is, with full self-consistent coupling to all higher multipole moments. The *dipole approximation* consists of truncating Eq. (32) just at the dipole level (i.e., $l_0 = 1$). This includes part of the local field effect, but the approximation remains largely inaccurate, because many more multipole moments are actually coupled when the particles are at close range or aggregate.

To understand the dependence of the yield stress and other generalized forces on the applied field E_0, we recall that all of the multipole moments induced on the individual particles are assumed to be linear in the local field [Eq. (30)], and that the coupled equations [Eq. (32)] are linear in the multiple moments. However, Eq. (32) also involves the system configuration, which is generally affected by the applied field (as well as shearing and other conditions). Therefore, the response of the system is generally a nonlinear function of the applied field, especially over a wide range. However, if the

system configuration is fixed, as in a solidified ER fluid, or reaches a steady-state equilibrium under shear flow, it becomes independent of E_0, and the dipole moments become proportional to E_0 even through the coupled Eq. (32). Then, the yield stress and other generalized forces become proportional to E_0^2 through Eq. (39) (the change in configuration is only infinitesimal therein). This by no means validates any dipolar approximation, which may also predict such quadratic dependence, because that still ignores coupling to higher multipoles and local field effects.

Now we discuss a few basic examples of exact results that can be obtained for different forms of single chains. In these numerical calculations, multipole moments up to $l_0 = 300$ and images up to $k = \pm 20$ have been included, with a corresponding estimated error below 1%. We consider identical spherical particles (hence, omit the particle index n) with a linear response in a core of radius a and dielectric constant ϵ_c and another linear response in a coating layer of outer radius b and dielectric constant ϵ_s. Because of symmetry, each multipolar component of the local potential can induce only one multipole moment of the same order on spherical particles. For coated spheres, the complete set of polarization coefficients is given by (76,85)

$$\lambda_{lm}^{l'm'} = \frac{1}{3} l(2l+1)\delta_l^{l'}\delta_m^{m'} b^{(2l+1)} \times \frac{(\epsilon_s - \epsilon_h)[l\epsilon_c + (l+1)\epsilon_s] + (\epsilon_c - \epsilon_s)[l\epsilon_h + (l+1)\epsilon_s]\left(\frac{a}{b}\right)^{(2l+1)}}{[l\epsilon_c + (l+1)\epsilon_s][l\epsilon_s + (l+1)\epsilon_h] + l(l+1)(\epsilon_c - \epsilon_s)(\epsilon_s - \epsilon_h)\left(\frac{a}{b}\right)^{(2l+1)}} \tag{42}$$

For a metal core, one can take the limit $\epsilon_c \to \infty$ in Eq. (42) and obtain

$$\lambda_{lm}^{l'm'} = \frac{1}{3}(2l+1)\delta_l^{l'}\delta_m^{m'} b^{(2l+1)} \times \frac{l(\epsilon_s - \epsilon_h) + [(l\epsilon_h + (l+1)\epsilon_s]\left(\frac{a}{b}\right)^{(2l+1)}}{[l\epsilon_s + (l+1)\epsilon_h] + (l+1)(\epsilon_s - \epsilon_h)\left(\frac{a}{b}\right)^{(2l+1)}} \tag{43}$$

For uniform spheres, one can immediately take $\epsilon_s = \epsilon_c$ (or let $a = b$) in Eq. (42).

The following numerical results have been obtained with $\epsilon_h = 1.0$ for simplicity. As units for the electric field and the particle outer radius, we use the typical values $E_0 = 1$ kV/mm and $b = 10$ μm. The corresponding forces are given in Figs. 3–7 in units of millidynes. Recalling that forces scale with E_0^2 for linear response and with b^2, if all distances in the system (including a) are scaled proportionally to b, force values for different fields and particle radii can be immediately obtained from the same figures. On the other hand, these calculations are confined to individual chains and their breaking at single points. Therefore, no precise value for any component of the yield stress tensor can be immediately obtained. However, dividing by the area 4×10^{-6} cm^2 of a particle diameter squared, we can estimate that a force of 100 millidynes translates into a yield stress tensile component of the order of 2.5 kPa, which agrees with stress values typically observed for $E_0 = 1$ kV/mm.

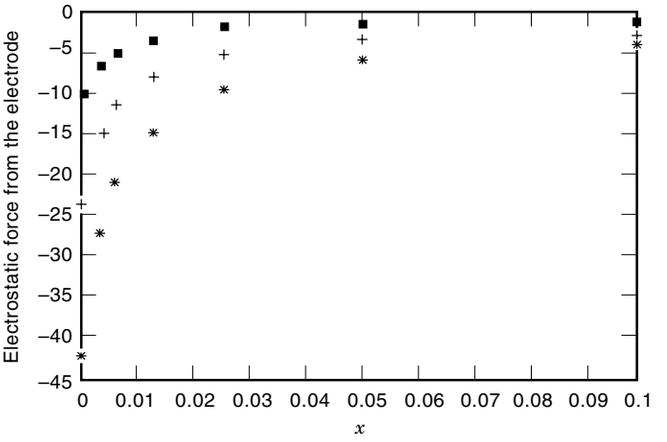

Figure 3. Electrostatic force between the left electrode and a single particle (solid squares), a two-particle chain (crosses), and a five-particle chain (asterisks), as functions of the distance (x) between the left electrode and the (leftmost) particle surface. The particles have a conducting core of radius $a = 0.95$, plus an insulating coating shell of outer radius $b = 1.0$ and dielectric constant $\epsilon_s = 10.0$. Force values are in millidynes for an electric field of 1 kV/mm and an outer radius of 10 μm.

Figure 3 shows the electrostatic force between one electrode and chains with various numbers of particles as a function of distance from the left electrode. The figure shows clearly that the images attract the particles toward the electrodes (the UEF model obviously cannot account for such attraction to the electrodes). Notice that the attractive force decreases rapidly as the distance from the electrode increases, a clear manifestation of the multipolar nature of the interactions.

Now we consider the crucial issue of the strength of the ER effect and its dependence on the properties of the ER fluid constituents. An indicator of such strength is the longitudinal force required to break a chain whose particles are in contact

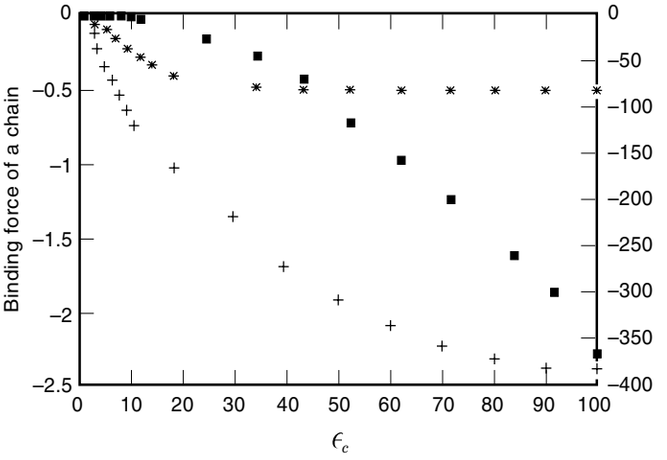

Figure 4. Binding force of a chain of uniform spheres of unit radius and dielectric constant ϵ_c, stretching between the two electrodes, as a function of ϵ_c. The left ordinates refer to the dipole (crosses) and fixed-dipole (asterisks) approximations, whereas the right ordinates refer to the exact results (solid squares).

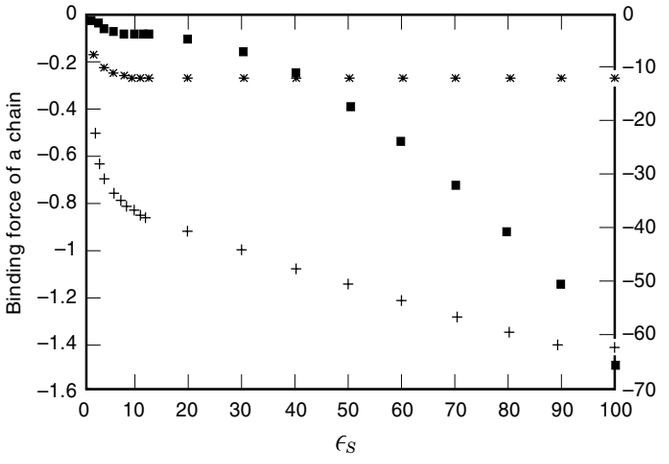

Figure 5. Binding force of a chain of spheres with an insulating core of radius $a = 0.95$ and dielectric constant $\epsilon_c = 10.0$, plus an insulating coating shell of outer radius $b = 1.0$, as a function of the coating dielectric constant ϵ_s.

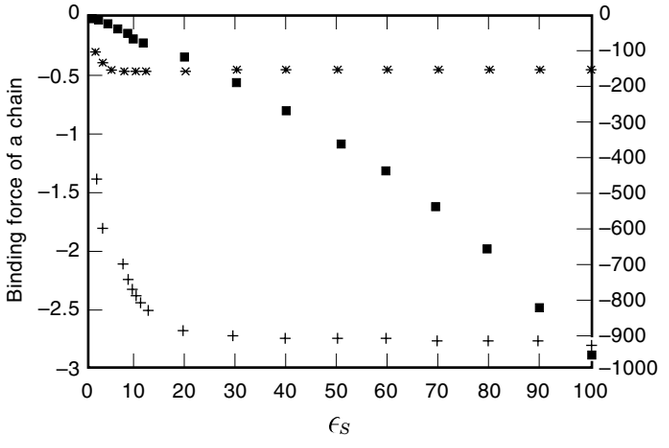

Figure 6. Same as Fig. 5 but for particles with a conducting core.

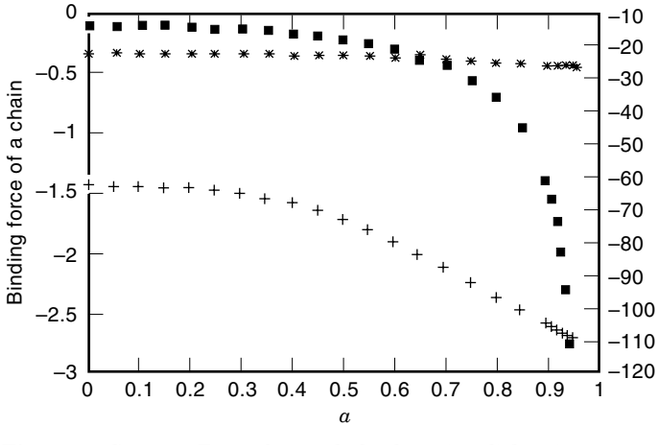

Figure 7. Same as Fig. 6, but with fixed coating dielectric constant $\epsilon_s = 20.0$ and varying core radius a.

and span the gap between the two electrode plates. Such a force, whose negative we call binding force, is directly related to the static tensile yield stress, except that a bundle of chains or a columnar structure should be considered in a more realistic microscopic configuration. Because of symmetry, the binding force is independent of the chain length and is the same for breaking the chain anywhere. On the other hand, the UEF model, lacking the images, yields binding forces that artificially weaken toward the chain ends (75). The experimental situation is more complicated. For example, one may observe that thin fibrils fracture in the middle, whereas thick columns break at the electrode (15, 70). This indicates (1) that surface adhesion plays an important role, and (2) that forces between chains are significant when they form thick columns. Surface adhesion may be included, at least phenomenologically, in the modeling and simulation of specific systems, and interchain electrical forces can be calculated accurately within the theoretical framework outlined (although no such calculations have yet been performed in detail).

Here we compute the binding force only in single chains of uniform spheres, spheres with a dielectric core and a dielectric coating layer, and spheres with a metal core and a dielectric coating layer. The corresponding results are plotted in Figs. 4–7.

Figure 4 shows that the ER effect for uniform spheres increases with *contrast,* which is the ratio between the dielectric constant of the particles and that of the medium. For coated dielectric spheres, Fig. 5 shows that the ER effect increases with the dielectric constant in the coating. This is consistent with the observation that activators with large dielectric constants surrounding the particles dramatically increase the ER effect, even when the particles themselves are not very ER active. Figure 6 shows that also for particles with a metal core, the larger the coating dielectric constant, the greater the ER effect. Figure 7 further shows that the thinner the coating layer (as long as it is adequate to keep the metal core insulated), the greater the ER effect.

These results demonstrate that the greatest binding force is obtained with coated metal spheres. This supports the search for anhydrous ER fluids based on conducting particles surrounded by thin and highly polarizable insulating shells. Note, however, that metal spheres with thick or low-polarizability coatings are still not particularly ER effective. This may be one of the reasons why insulated metal particles have not yet conclusively demonstrated substantial ER activity independent of water (37).

Improved stability against gravitational and centrifugal settling is attained by reducing the weight of structured particles. Thus, one may fabricate doubly coated spheres, consisting of a light dielectric core, a thin metal coating, and an outer dielectric coating (still needed to prevent conduction through the system) (31,32). At least at low frequencies, the electrostatic interactions among such doubly coated spheres should be independent of the core material. In fact, they should be the same as those of singly coated metal spheres (29,30), because the metal layer completely screens the penetration of the electric field into the inner core, and thus the polarization coefficients are the same as in Eq. (43).

Figures 4–7 clearly show that the fixed-dipole (asterisks) and the dipole (crosses) approximations underestimate by two or more orders of magnitude the value of the binding force, a fact typically confirmed by comparison with experiments (14,

15, 21, 86, 87). and even fail to describe the correct trends. In fact, the dipole approximations exhibit systematic *saturation,* as expected from the dipolar polarization coefficient λ_{10}^{10}, which saturates when ϵ_c and ϵ_s increase. However, the exact binding force never saturates, and grows faster with increasing ϵ_c and ϵ_s, as higher and higher multipoles contribute. Experiments have shown that the ER effect does not saturate with increasing particle–medium dielectric mismatch, contrary to dipole predictions (87). Our exact calculations demonstrate that the surprising strength of ER fluids indeed depends by and large on the multipolar interactions among the particles.

As already noted, Eq. (39) shows that a large electrostatic force requires a large *variation* of the system's total dipole moment in response to a (virtual) change of microscopic configuration, rather than a large absolute value of the total dipole moment itself. That occurs only if the dipole moments of the particles are strongly coupled (through the local field) to many higher multipolar terms, because only those change rapidly with the change of distance among the particles. Thus, only in systems with strong multipolar interactions, hence, sufficiently large polarization coefficients of higher orders, the total induced dipole moment, hence, the interaction energy, is very sensitive to the change of microscopic configuration. Systems with limited multipolar interactions should not be expected to exhibit a strong ER effect, even if the dipole moments of the particles are very large. Experiments indeed suggest that ER activity correlates with interfacial, rather than orientational polarization. This may explain why systems with ferroelectric particles do not necessarily yield significant ER activity when rigorously dried, despite the large dielectric constant of the particles. For example, a system of TiO_2 particles in paraffin oil completely loses its ER activity if carefully dried (27, 37), even though TiO_2 is an incipient ferroelectric with a dielectric constant between 70 and 200 (depending on the precise structure). The same occurs with electrets, that is, particles with attached permanent dipoles. However, other experiments indicate that ferroelectric particles may very well exhibit strong ER activity, increasing with the particle–medium dielectric mismatch, without saturation (87). That definitely indicates strong multipolar polarization coefficients, possibly resulting from a different ferroelectric domain structure or perhaps aided by even minimal water surroundings.

The prototypical examples provided previously serve only as illustrations. However, complete and accurate computations of realistic systems and configurations based on this method are entirely feasible, although obviously much more demanding. For a system of n_0 particles and required highest order l_0 of multipole moments, one has to solve for n_0 dipole moments q_{n1m} in a set of N linear Eqs. (32), where

$$N = n_0 \sum_{l=1}^{l_0} (2l + 1) = n_0 l_0 (l_0 + 2) \tag{44}$$

For systems with symmmetry, N can be significantly reduced. For example, ground-state structures, static yield stress, interactions between pair of chains, and other ordered properties can be determined exactly with only moderate computation. On the other hand, full implementation of multipolar interactions in computer simulations of dynamic configurations and evolution, which also require a large number of particles, may very well need super or parallel computing resources. However, this is also the case for other presently developing fields in computational physics. Therefore, complete theoretical understanding and predictive computation of ER phenomena and materials may be attained in the near future.

BIBLIOGRAPHY

1. W. M. Winslow, *Methods and means for translating electrical impulses into mechanical force,* U.S. Patent No. 2,417,850, 1947.
2. W. M. Winslow, Induced fibration of suspensions, *J. Appl. Phys.,* **20**: 1137–1140, 1949.
3. W. König, Bestimmung einiger Reibungscoëfficienten und Versuche über den Einfluss der Magnetisirung und Electrisirung auf die Reibung der Flüssigkeiten (Determination of some friction coefficients and investigation of the influence of magnetization and electrification on the friction of the fluids), *Ann. Phys. (Leipzig),* **25**: 618–625, 1885.
4. A. W. Duff, The viscosity of polarized dielectrics, *Phys. Rev.,* **4**: 23–38, 1896.
5. G. Quincke, Die Klebrigkeit isolirender Flüssigkeiten im constanten electrischen Felde (The stickiness of insulating fluids in a constant electric field), *Ann. Phys. Chem.,* **62**: 1–13, 1897.
6. K. D. Weiss, J. D. Carlson, and J. P. Coulter, Material aspects of ER systems, *J. Intell. Mater. Syst. Struct.,* **4**: 13–34, 1993; also in Ref. 7, pp. 30–52.
7. M. A. Kohudic (ed.), *Advances in Electrorheological Fluids,* Lancaster, PA: Technomic, 1994.
8. J. D. Carlson, *Surfactant-based ER materials,* U.S. Patent No. 5,032,307, 1991.
9. H. Conrad, M. Fisher, and A. F. Sprecher, Characterization of the structure of a model ER fluid employing stereology, *Proc. 2nd Int. Conf. ER Fluids,* Raleigh, NC, 1989, 1990, pp. 63–81.
10. J. C. Hill and T. H. van Steenkiste, Response times of ER fluids, *J. Appl. Phys.,* **70**: 1207–1211, 1991.
11. See Fig. 3 of Ref. 6 and Fig. 3 of H. Conrad and Y. Chen, Electrical properties and the strength of ER fluids, *Proc. Am. Chem. Soc. Symp. ER Mater. Fluids,* Washington, DC, 1994, 1995, pp. 55–85.
12. J. E. Stangroom, ER fluids, *Phys. Technol.,* **14**: 290–296, 1983.
13. M. T. Shaw and R. C. Kanu, ER fluids (role of polymers as the dispersed phase), in J. C. Salamone (ed.), *Polymeric Materials Encyclopedia,* New York: CRC Press, 1996, vol. 3, pp. 2023–2028.
14. R. C. Kanu and M. T. Shaw, Effect of dc and ac electric fields on the response of ER fluids comprising cylindrical PBTZ particles, *Proc. Am. Chem. Soc. Symp. ER Mater. Fluids,* Washington, DC, 1994, 1995, pp. 303–323.
15. T. Jordan, M. T. Shaw, and T. C. B. McLeish, Viscoelastic response of ER fluids. II. Field strength and strain dependence, *J. Rheol.,* **36** (3): 441–463, 1992.
16. T. J. Chen, R. N. Zitter, and R. Tao, Laser diffraction determination of the crystalline structure of an ER fluid, *Phys. Rev. Lett.,* **68**: 2555–2558, 1992.
17. J. E. Martin, J. Odinek, and T. C. Halsey, Evolution of structure in a quiescent ER fluid, *Phys. Rev. Lett.,* **69**: 1524–1527, 1992.
18. T. C. Halsey, ER fluids, *Science,* **258**: 761–766, 1992.
19. T. C. Halsey and J. E. Martin, ER fluids, *Sci. Amer.,* **269**: 58–64, 1993.
20. P. S. Neelakanta, *Handbook of Electromagnetic Materials,* Boca Raton, FL: CRC Press, 1995, chap. 24, pp. 527–548.
21. T. C. Jordan and M. T. Shaw, Electrorheology, *MRS Bull.,* **16** (8): 38–43, 1991.

22. R. E. Rosenweig, *Ferrohydrodynamics,* Cambridge, UK: Cambridge Univ. Press, 1985.
23. *Proc. 6th Int. Conf. ER Fluids, MR Suspensions Their Applications,* Yonezawa, Japan, 1997, to be published.
24. W. A. Bullough (ed.), *Proc. 5th Int. Conf. ER Fluids, MR Suspensions, Associated Technol.,* Singapore: World Scientific, 1996.
25. J. E. Stangroom, *Electric field responsive fluids,* U.S. Patent No. 4,129,513, 1978; *Improvements in or relating to electric field responsive fluids,* G.B. Patent No. 1,570,234, 1980.
26. L. M. Carreira and V. S. Mihajlov, *Recording apparatus and methods employing photoelectroviscous ink,* U.S. Patent No. 3,553,708, 1971.
27. F. E. Filisko, Overview of ER technology, *Proc. Am. Chem. Soc. Symp. ER Mater. Fluids,* Washington, DC, 1994, 1995, pp. 3–18; Materials aspects of ER fluids, in *Electrorheological Fluids: A Research Needs Assessment,* Washington, DC: Natl. Tech. Inf. Service, 1993, sec. 5.9.
28. H. Block and J. P. Kelly, *ER fluid containing continuous phase halogenated aromatic liquid and semiconductor or unsaturated fused polycyclic compound or a poly(acene-quinone) polymer as disperse phase functioning when anhydrous,* U.S. Patent No. 4,687,589, 1987.
29. A. Inoue, Study of new ER fluid, *Proc. 2nd Int. Conf. ER Fluids,* Raleigh, NC, 1989, 1990, pp. 176–183.
30. W. C. Yu et al., Design of anhydrous ER suspensions based on I_2-doped poly(pyridinium salt), *J. Polym. Sci. B,* **32**: 481–489, 1994.
31. A. Inoue, *New electroviscous fluid used for electrical controls, prepared by dispersing dielectric fine particles containing core organic solid particle, conductive- and outer-film layers, in oil medium,* JP Patent No. 63,097,694, 1988.
32. M. Prendergast, *ER fluids,* EP Patent No. 396,237, 1990.
33. Y. Ishino et al., *Electroviscous fluid with anhydrous carbon particulates, dispersed in insulating oil usable over wide temperature range, with low power consumption and with AC or DC,* EP Patent No. 361106, 1990; U.S. Patent No. 5,087,382, 1992; also see *Proc. Am. Chem. Soc. Symp. ER Mater. Fluids,* 1994, 1995, pp. 137–146.
34. F. E. Filisko and W. H. Armstrong, *Electric field dependent fluids,* U.S. Patent No. 4,744,914, 1988; U.S. Patent No. 4,879,056, 1989.
35. F. E. Filisko and L. H. Radzilowski, An intrinsic mechanism for the activity of aluminosilicate based ER materials, *J. Rheol.,* **34** (4): 539–552, 1990.
36. U. Y. Treasurer, F. E. Filisko, and L. H. Radzilowski, Polyelectrolytes as inclusions in ER active materials: Effect of chemical characteristics on ER activity, *J. Rheol.,* **35** (6): 1051–1068, 1991.
37. F. E. Filisko, Rheological properties and models of dry ER materials, *Proc. 3rd Int. Conf. ER Fluids,* Carbondale, IL, 1991, 1992, pp. 116–128.
38. J. D. Carlson, *Water-free ER fluid: Has dispersed particulate phase of lithium hydrazinium sulfate and dielectric liquid phase, e.g., silicone oil,* U.S. Patent No. 4,772,407, 1988.
39. K. Wissbrun, Potential application of liquid crystals as ER fluids, in *Electrorheological Fluids: A Research Needs Assessment,* Washington, DC: Natl. Tech. Inf. Service, 1993, sect. 5.10.
40. I-K. Yang and A. D. Shine, Electrorheology of a nematic poly(n-hexyl isocyanate) solution, *J. Rheol.,* **36** (6): 1079–1104, 1992.
41. B. R. Powell, *Preparation of ER fluids using fullerenes and other crystals having fullerene-like anisotropic electrical properties,* U.S. Patent No. 5,445,759, 1995.
42. U.S. Department of Energy, Office of Energy Research, *Electrorheological Fluids: A Research Needs Assessment,* Final Report, DOE/ER/30172, Washington, DC: Natl. Tech. Inf. Service, 1993.
43. H. Block and J. P. Kelly, Electrorheology, *J. Phys. D,* **21**: 1661–1677, 1988.
44. J. R. Wilson, ER fluid devices and energy savings, in *Electrorheological Fluids: A Research Needs Assessment,* Washington, DC: Natl. Tech. Inf. Service, 1993, sect. 5.1.
45. J. W. Pialet and D. R. Clark, The dependence of shear stress and current density on temperature and field for model ER fluids, *Proc. Am. Chem. Soc. Symp. ER Mater. Fluids,* Washington, DC, 1994, 1995, pp. 251–262.
46. R. C. Kanu and M. T. Shaw, Studies of ER fluids featuring rodlike particles, *Proc. 5th Int. Conf. ER Fluids, MR Suspensions, Assoc. Technol.,* Sheffield, UK, 1995, 1996, pp. 92–99.
47. J. P. Coulter, K. D. Weiss, and J. D. Carlson, Engineering applications of ER materials, *J. Intell. Mater. Syst. Struct.,* **4**: 248–259, 1993; also in M. A. Kohudic (ed.), *Advances in Electrorheological Fluids,* Lancaster, PA: Technomic, 1994, pp. 64–75.
48. R. Tao and G. D. Roy (eds.), *Proc. 4th Int. Conf. ER Fluids,* Singapore: World Scientific, 1994.
49. R. Tao (ed.), *Proc. 3rd Int. Conf ER Fluids,* Singapore: World Scientific, 1992.
50. J. D. Carlson, A. F. Sprecher, and H. Conrad (eds.), *Proc. 2nd Int. Conf. ER Fluids,* Lancaster, PA: Technomic, 1990.
51. H. Conrad, J. D. Carlson, and A. F. Sprecher (eds.), *Proc. 1st Int. Symp. ER Fluids,* Raleigh, NC: Univ. Eng. Publ., 1989.
52. K. O. Havelka and F. E. Filisko (eds.), *Progress in Electrorheology: Science and Technology of ER Materials; Proc. Am. Chem. Soc. Symp. ER Materials and Fluids,* New York: Plenum, 1995.
53. D. A. Siginer and G. S. Dulikravich (eds.), *Developments in ER Flows,* New York: Amer. Soc. Mech. Eng., 1995.
54. D. A. Siginer et al. (eds.), *Developments in ER Flows and Measurement Uncertainty,* New York: Amer. Soc. Mech. Eng., 1994.
55. T. R. Weyenberg, J. W. Pialet, and N. K. Petek, The development of ER fluids for an automotive semi-active suspension system, *Proc. 5th Int. Conf. ER Fluids, MR Suspensions, Assoc. Technol.,* Sheffield, UK, 1995, 1996, pp. 395–403.
56. N. K. Petek, R. J. Goudie, and F. B. Boyle, Actively controlled damping in ER fluid-filled engine mounts, *Proc. 2nd Int. Conf. ER Fluids,* Raleigh, NC, 1989, 1990, pp. 409–418.
57. E. V. Korobko, The state of the art of ER studies in the former USSR, in *Electrorheological Fluids: A Research Needs Assessment,* Washington, DC: Natl. Tech. Inf. Service, 1993, sect. 6.1.
58. A. L. Fetter and J. D. Walecka, *Theoretical Mechanics of Particles and Continua,* New York: McGraw-Hill, 1980.
59. L. D. Landau and E. M. Lifshitz, *Fluid Mechanics,* 2nd ed., vol. 6, Oxford: Pergamon and Butterworth-Heinemann, 1987.
60. L. D. Landau and E. M. Lifshitz, *Theory of Elasticity,* 3rd ed., vol. 7, Oxford: Pergamon and Butterworth-Heinemann, 1986.
61. W. L. Wilkinson, *Non-Newtonian Fluids,* New York: Pergamon, 1960.
62. H. A. Barnes, J. F. Hutton, and K. Walters, *An Introduction to Rheology,* Amsterdam: Elsevier, 1989.
63. T. E. Faber, *Fluid Dynamics for Physicists,* Cambridge, UK: Cambridge Univ. Press, 1995, chap. 10.
64. J. W. Goodwin, Rheological characterization of ER fluids, in *Electrorheological Fluids: A Research Needs Assessment,* Washington, DC: Natl. Tech. Inf. Service, 1993, sect. 5.6.
65. D. R. Gamota and F. E. Filisko, Dynamic mechanical study of ER materials: Moderate frequencies, *J. Rheol.,* **35** (3): 399–425, 1991.
66. D. R. Gamota and F. E. Filisko, High frequency dynamic mechanical study of an aluminosilicate ER material, *J. Rheol.,* **35** (7): 1411–1424, 1991.
67. T. C. B. McLeish, T. Jordan, and M. T. Shaw, Viscoelastic response of ER fluids. I. Frequency dependence, *J. Rheol.,* **35** (3): 427–448, 1991.
68. A. B. Metzner, Fluid mechanics, in *Electrorheological Fluids: A Research Needs Assessment,* Washington, DC: Natl. Tech. Inf. Service, 1993, sect. 5.7.

69. H. A. Pohl, *Dielectrophoresis: The Behavior of Neutral Matter in Nonuniform Electric Fields,* Cambridge, UK: Cambridge Univ. Press, 1978.

70. T. C. Jordan and M. T. Shaw, Structure in ER fluids, *Proc. 2nd Int. Conf. ER Fluids,* Raleigh, NC, 1989, 1990, pp. 231–251.

71. Y. Chen, A. F. Sprecher, and H. Conrad, Electrostatic particle-particle interactions in ER fluids, *J. Appl. Phys.,* **70**: 6796–6803, 1991.

72. R. Friedberg and Y. K. Yu, Energy of an ER solid calculated with inclusion of higher multipoles, *Phys. Rev. B,* **46**: 6582–6585, 1992.

73. H. J. H. Clercx and G. Bossis, Many-body electrostatic interactions in ER fluids, *Phys. Rev. E,* **48**: 2721–2738, 1993.

74. H. J. H. Clercx and G. Bossis, Electrostatic interactions in slabs of polarizable particles, *J. Chem. Phys.,* **98**: 8284–8293, 1993.

75. L. Fu and L. Resca, Exact treatment of the electrostatic interactions and surface effects in ER fluids, *Phys. Rev. B,* **53**: 2159–2198, 1996.

76. L. Fu and L. Resca, Exact theory of the electrostatic interaction in ER fluids and the effects of particle structure, *Solid State Commun.,* **99**: 83–87, 1996.

77. J. D. Jackson, *Classical Electrodynamics,* 2nd ed., New York: Wiley, 1975.

78. C. F. Zukoski, Mechanisms of ER effects, in *Electrorheological Fluids: A Research Needs Assessment,* Washington, DC: Natl. Tech. Inf. Service, 1993, sect. 5.3.

79. A. M. Kraynik, Modeling and simulation of ER fluids, in *Electrorheological Fluids: A Research Needs Assessment,* Washington, DC: Natl. Tech. Inf. Service, 1993, sect. 5.5.

80. P. L. Taylor, Cooperative aspects of ER phenomena, in *Electrorheological Fluids: A Research Needs Assessment,* Washington, DC: Natl. Tech. Inf. Service, 1993, sect. 5.4.

81. L. Fu and L. Resca, Analytic approach to the interfacial polarization of heterogeneous systems, *Phys. Rev. B,* **47**: 13818–13829, 1993.

82. L. Fu and L. Resca, Electrical response of heterogeneous systems with inclusions of arbitrary structure, *Phys. Rev. B,* **49**: 6625–6633, 1994.

83. L. Fu, Electrical response of heterogeneous systems of nonlinear inclusions, *Phys. Rev. B,* **51**: 5781–5789, 1995.

84. L. D. Landau and E. M. Lifshitz, *Electrodynamics of Continuous Media,* 2nd ed., vol. 8, Oxford: Pergamon and Butterworth-Heinemann, 1984, sec. 11, chap. 2.

85. L. Fu and L. Resca, Optical response of arbitrary clusters of structured particles, *Phys. Rev. B,* **52**: 10815–10818, 1995.

86. A. P. Gast and C. F. Zukoski, ER fluids as colloidal suspensions, *Adv. Colloid Int. Sci.,* **30**: 153–202, 1989.

87. T. Garino, D. Adolf, and B. Hance, The effect of solvent and particle dielectric constants on the ER properties of water-free ER fluids, *Proc. 3rd Int. Conf. ER Fluids,* Carbondale, IL, 1991, 1992, pp. 167–174.

LIANG FU
LORENZO RESCA
Catholic University of America

ELECTROSTATIC CHARGES. See ELECTROSTATIC PROCESSES.